DESIGN AND IMPLEMENTATION OF A LOW POWER, LOW COST S-BAND BISTATIC RECEIVER

By

Benjamín De Jesús Castro

A project submitted in full fulfillment of the requirements for the degree of

MASTER OF ENGINEERING

in

ELECTRICAL ENGINEERING

UNIVERSITY OF PUERTO RICO

MAYAGÜEZ CAMPUS

2012

Approved by:

Sandra L. Cruz-Pol, PhD Member, Graduate Committee	Date
Rafael Rodríguez Solís, PhD Co-President, Graduate Committee	Date
José G. Colom Ustáriz, PhD President, Graduate Committee	Date
Dorial Castellanos, PhD Representative of Graduate Studies	Date
Pedro I. Rivera-Vega, PhD Chairperson of the Department	Date

ABSTRACT

This document summarizes the design, fabrication, and testing of an S-band receiver single node for a multistatic radar network application. The proposed receiver design established the need of low cost, low power, easy to replicate and deploy system, to be operated by the United States Air Force. This work has been completed by modifying a previous prototype receiver built under the same USAF grant at Colorado State University with UPRM collaboration. The modifications consist in the replacements of the most expensive components including the antenna, the data acquisition system, the synchronization system, the containing box and adjustments to the operating frequency bandwidth. Presented as part of the design are tests to individual components, sub-systems and to the complete receiver as a system. With the modifications made to the existing receiver the cost has been reduced approximately by a factor of 4. In addition, a solar energy option was implemented for the modified design.

RESUMEN

En este documento se resume el trabajo hecho para crear un recibidor de radar como nodo de una red de recibidores que formaran un sistema de radar multiestatico para la Fuerza Aérea de los Estados Unidos. El recibidor propuesto responde a la necesidad de un sistema de bajo costo, bajo consumo de potencia y fácil de duplicar e instalar para ser operado por la Fuerza Aérea de los Estados Unidos. Esto se logró modificando un recibidor ya creado y entregado hecho en la Universidad del Estado de Colorado en colaboración con la Universidad de Puerto Rico recinto de Mayagüez. Las modificaciones hechas son básicamente el remplazo o modificación de los componentes o sub- sistemas más caros, como la antena, el sistema de adquisición de datos, el sistema de sincronización, la caja que contiene el sistema y la modificación del ancho de banda del sistema. Con las modificaciones hechas al sistema se logró reducir aproximadamente 4 veces el costo del recibidor original. Un sistema de potencia solar se ha implementado en este diseño modificado.

To the All . . .

ACKNOWLEDGEMENTS

During my studying years at the University of Puerto Rico at Mayagüez, several people contributed to the completion of this project. Directly or indirectly they helped me finish my work and this section is to recognize them and tell them that without them I would not have been able to finish.

First of all I want to thank God for the courage and strength He gave me all this time. To my family for your support, guidance and understanding, even when there were a lot of family activities that I miss for being working on this, you always supported me and never changed your attentions to me.

I want to thank Dr. José Colom and Dr. Sandra Cruz-Pol for giving me the opportunity to do research since undergraduate and allow me to continue to graduate school, your attentions, support and guidance are unbeatable. I always will be in your debt. Special thanks to Dr. Rafael Rodriguez Solis for being there always that I needed some academic guidance.

A very special appreciation to Professor Madeline Rodriguez, for being there when I needed to talk to somebody and most of all for guiding me through the university life, without you I am sure that I would not finished my university career. Also I want to thank her team, “Team Made”.

Last but not least I want to thank all members of the CLiMMATE laboratory, the past and the present ones, your help, support and knowledge has made this happen. Inside the group, that I will not mention not to let anybody out, I want to give special thanks to two persons; Jose Ortiz, a.k.a. “Kotshie”, for your help in everything software related, without your help the

software would be, more than a mess, a disaster, and to Jose Rosario, I owe you, for being a great partner working with the radars, travelling in and out of Puerto Rico, to do work or simply being there helping when it was not your duty and for being a better friend.

Table of Contents

ABSTRACT II

RESUMEN II

RESUMEN III

ACKNOWLEDGEMENTS V

TABLE OF CONTENTS VII

TABLE LIST IX

FIGURE LIST X

1 INTRODUCTION 2

1.1 MOTIVATION 2
1.2 OBJECTIVES 4
1.3 PROJECT DESCRIPTION 5
1.4 LITERATURE REVIEW 6
1.4.1 Advantages and Disadvantages of multistatic systems *7*
1.4.2 Bistatic Radar Classes *8*
1.4.3 Multistatic Radar Operation Modes *9*
1.5 SUMMARY OF FOLLOWING CHAPTERS 10

2. THEORETICAL BACKGROUND 12

2.1 RADAR THEORY 12
2.1.1 Noise and Dynamic Range *13*
2.1.2 Bistatic Radar *16*
2.1.3 Bistatic radar Synchronization *18*
2.1.4 Bistatic Doppler *20*
2.1.5 Cassini Ovals *21*
2.1.6 Bistatic Radar Cross Section *22*
2.2 ANTENNA THEORY 23
2.2.1 Microstrip Antennas *23*
2.2.2 Antenna Gain and Radiation Pattern *25*
2.2.3 Antenna Polarization *27*
2.2.4 Antenna Array *29*

3 SYSTEM DESIGN 30

3.1 PURPOSE 30
3.2 RF OPERATION 30
3.3 DATA ACQUISITION SYSTEM 32
3.4 SOLAR CIRCUIT 35
3.5 ANTENNA 36
3.5.1 Simulation Software *36*
3.5.2 Antenna Design *37*

4 TEST AND CONSTRUCTION 44

4.1 COMPONENTS 44
4.2 RF CHARACTERIZATION 45

4.3 DATA ACQUISITION SYSTEM 48
4.4 ANTENNA 50
4.4.1 Antenna Construction..*50*
4.5 INTEGRATION AND IMPLEMENTATION..59

5 CONCLUSION AND FUTURE WORK 64

APPENDIX A. SOLAR CALCULATION TABLES 69

APPENDIX B C++ PROGRAM FOR ADLINK PCI-9812 73

APPENDIX C GPS REFERENCE SPECIFICATIONS 78

1. QUARTZLOCK PRODUCTS 78

a. E8-X *78*
ii. Standard Specification: *79*

Table List

Tables	Page
Table 1 Advantages and Disadvantages of Multistatic systems [5&6]	7
Table 2 Bistatic radar application according to location and configuration.	10
Table 3 Monostatic set of equations	13
Table 4 Bistatic radar equation	17
Table 5 Microstrip antenna patch design equations	25
Table 6 Studied data acquisition cards	33
Table 7 Antenna Calculated Dimensions	38
Table 8 Components price and comparison	45
Table 9 RF Components characterization	48

Figure List

Figures **Page**

Figure 1. Receiver Stand ... 5
Figure 2 Bistatic angle and Range description ... 9
Figure 3 Radar Block Diagram [9] ... 12
Figure 4 Receiver dynamic range example ... 16
Figure 5 Bistatic radar geometry ... 17
Figure 6 Cassini oval example ... 22
Figure 7 Microstrip Antenna ... 24
Figure 8 Antenna radiation patterns [24] ... 27
Figure 9 Illustration of linear and circular polarization [28] ... 28
Figure 10 Antenna Array ... 29
Figure 11 Receiver Block Diagram ... 31
Figure 12 Computer and Data Acquisition Board ... 35
Figure 13 S11 or return loss for a single square patch ... 39
Figure 14 Single patch gain ... 40
Figure 15 Selected antenna array configuration ... 41
Figure 16 Return loss for the complete array ... 41
Figure 17 Complete antenna array gain ... 42
Figure 18 S21 or port isolation for the complete antenna array ... 43
Figure 19 RF Components at the aluminum plate ... 46
Figure 20 Receiver Characterization Setup ... 47
Figure 21 100KHz signal at 0dBm as plotted by PCI-9812 ... 49
Figure 22 25MHz modulated by a 10KHz signal ... 50
Figure 23 Antenna in CircuitCam ... 51
Figure 24 BoardMaster window ... 52
Figure 25 Antenna in progress ... 53
Figure 26 Antenna Completed ... 54
Figure 27 Horizontal polarization return loss ... 55
Figure 28 Vertical polarization return loss ... 55
Figure 29 Antenna port isolation ... 56
Figure 30 Antenna inside cover ... 56
Figure 31 Vertical polarization return loss. (Antenna in cover) ... 57
Figure 32 Horizontal polarization return loss. (Antenna in cover) ... 58
Figure 33 Antenna port isolation (Antenna in cover) ... 58
Figure 34 Stand with antenna, weather proof box and solar panel. ... 59
Figure 35 Receiver Completed ... 60
Figure 36 Transmitter antenna used for the final test ... 60
Figure 37 Transmitter's location during receiver test ... 61
Figure 38 Receiver with the transmitter off ... 62

Figure 39 Transmitting horizontal polarization only 62
Figure 40 Transmitting Vertical polarization only 62
Figure 41 Transmitting horizontal and vertical at the same time 63

1 INTRODUCTION

1.1 Motivation

A simple way to explain how a radar works is visualizing a system that transmits a radio frequency wave through an antenna, this wave hits an object or target and part of that wave reflects and reaches the radar antenna, where signal processing is performed to interpret the received signal and identify different parameters of the object. A radar system can have more than one antenna, when the receiver and transmitter antenna is the same it is called a monostatic radar. In contrast, when the receiver antenna or antennas are considerably apart from the transmitter the system is called a multistatic radar.

Radars are designed to acquire information from a target by understanding how the wave has been affected by interfering with the object under observation. Nowadays the military technology developers are dedicated to make devices to remain undetected under enemy radars, or to become "invisible". They are close to the objective, developing missiles and all kind of military vehicles invisible to the common radars. These technologies use materials and shapes that cause the incident radar wave to attenuate and/or disperse in every direction instead of using typical construction techniques with materials and shapes that reflects most of the wave power back to the radar.

The first radars ever created were bistatic systems [1], which are a multistatic system with just one antenna for receiving and one antenna for transmitting. But because of the convenience of having a monostatic system, the bistatic radar rapidly lose interest from the scientific community. The main difference between the two receivers is that the monostatic system received the bounced back signal from the target while the bistatic captures the signal bounced in other directions, depending on the location with respect to the object and the sending radar transmitter.

The main challenge for the militarized countries, with the increase in stealth technology, is to been able to "see" or detect the "invisible" target using radars. Since the powerful signal of the transmitting part of the radar is not present in the bistatic receiver, the receiver circuit can be more sensitive, sensing the attenuated signal of the stealth technology, and also because of its different location it can detect the deviated RF signal from the target. This knowledge increased the interest again in the development of bistatic radars. The United States Air Force (USAF) is one of the agencies with interest in developing a multistatic radar system network. The transmitters and receivers in this type of network can consist of combinations of monostatic radars and/or independent transmitters and receivers. In this project, the USAF opted to use their existing S-band radar network and design new receivers to sparse them around the radars modifying it into multistatic networks. A prototype receiver was already developed by UPRM and Colorado State University (CSU) and delivered to USAF. This was the first goal achieved for this project. The purpose in the continuation of this project is to develop a similar receiver with a much smaller budget and provide an option of solar energy operation.

1.2 Objectives

The main objective of this project is to design, construct and test an easy to deploy and to duplicate radar receiver. This receiver will be similar to the one developed in CSU with the collaboration of UPRM, but at a much less cost. Performance will be limited in terms of bandwidth and capabilities since the high data rate and broad bandwidth acquisition card used in the original prototype will be replaced, also the antenna will be a microstrip in-house design that will not have the bandwidth of a more costly commercially available horn antenna. In addition, as part of the final goal, an Operator's Manual will be developed for the end user. In order to work with the existing USAF S-band radar, the receiver has to have the following characteristics:

- Operate at S-Band (2 to 4 GHz)*
- Antenna and RF circuit capable of receive dual-polarization signal.
- Doppler capability. This means that the receiver should be capable to detect the magnitude and phase of the received signal

In order to comply with the end user requirements the system must be:

- Easy to replicate, to add multiple receivers to the system.
- Easy to carry, deploy, configure and manage.
- Low power consumption so it can be used with renewable power source.
- Low cost device since it will be part of a network and therefore the use of many of these devices will be required.

- In order for the receiver to work as a network it must have the capability to synchronize with other units.

- It must have an option to determine its exact position and give a very precise time.

1.3 Project Description

The receiver is mounted in a four feet height stand, as seen in Figure 1, with bars on the top and bottom which are two and a half feet wide. This stand is completely detachable and the antenna part of the stand provides two rotational axes, giving this way the capability to the user to select an operational angle in azimuth and elevation. On the top of this stand are mounted two antennas, one for the RF signal and the other a GPS antenna for synchronization purposes. In the vertical pole of the stand a weather proof box with all the circuitry of the receiver is attached. The system works with solar power, the solar panel is also mounted in the vertical pole , opposite to the weather proof box, and the battery and charge controller are in the inside cover part of the box door.

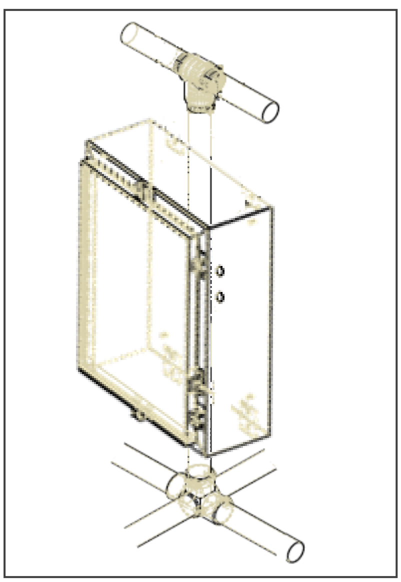

Figure 1. Receiver Stand

1.4 Literature Review

Bistatic radars have been around since the radar origins in the 1920’s, at that time this particular mode of operation was the predominant in radar systems. Radar appeared almost simultaneously in the United States, United Kingdom, France, Italy, Russia and Japan. In the United States the first bistatic radar was used in 1922 when A. Taylor and L.C. Young of the US Naval Research Laboratory detected a wooden ship. In late 1930s and through WWII there is evidence of the usage of various bistatic radar systems that helps different countries to defend itself against air attacks [2]. But after the development of the duplexer, a device invented at the US Naval Research Laboratory in 1936 [3] that allows a single antenna to be used as a transmitter and receiver at the same time; the monostatic radar interest significantly increased, leaving the bistatic systems reserved just when it is strictly necessary. Since the radar invention, improvements and development was mostly a military secret operation, is not until 1978 with the publication of Dispersed Radar Stations and Systems authored by V.Ya. Aver’yanov, that there is a textbook on bistatic radar systems available. The published paper was machine translated in English in 1980 but never distributed outside the United States government agencies [1]. For this reason, the literature in bistatic radar is very limited compared to monostatic radar. But it has been remarked that interest in bistatic radar has varied cyclically, with a period of approximately 15 years. As stated before, the first radars used were bistatic in the middle 1930s, then in the 1950s they emerged with the development of semi-active homing missiles and systems. Later in the late 1970s and early 1980s they resurge as multistatic systems with an application known as hitchhikers, later explained in section 1.4.3, and then in the mid 1990 with the development of the passive bistatic radar. After the last resurgence, it is arguably said that it has not ended because of the many practical systems demonstrations, especially with the availability of the GPS which solves the synchronization problem with the multistatic radar. [4].

1.4.1 Advantages and Disadvantages of multistatic systems

Depending on the desired application these radar systems will have advantages and disadvantages. These are presented in form of a table below. Price is not listed in the table since it is relative to variations from parameters such as range, sensitivity and scan capability

Advantages	**Disadvantages**
Improves target location accuracy	Geometry more complicated, compared to monostatic systems.
Reduces target glint	It is necessary to provide some form of synchronization between transmitter and receiver.
Covert operation against emitter locators, jammers and anti-radiation missiles	Very high probability of use “pulse chasing” processing.
Covertly detect stealthy vehicles in their RCS resonance region	Doppler shift depends on the motion of target, transmitter and receiver which make the equation quite complicated.
Countering high gain, retrodirective jamming by locating the receiver outside the retro-jammer’s main beam	Totally dependent of a friendly or hostile illumination source for operation.
Avoid dedicated transmitter volume, weight, and cost penalties in the radar system	
Receiving systems are potentially simple and cheap	

Table 1 Advantages and Disadvantages of Multistatic systems [5&6]

1.4.2 Bistatic Radar Classes

Generally, there are four classes of bistatic radars. These four specific classes include [7]:

- **Pseudo-monostatic radar** is a radar system where the bistatic angle, β, (angle made between the transmitter antenna, the receiver antenna and the target) is very close to zero.
- **Forward scatter radar** is the bistatic radar that is designed to operate in a fence-like configuration, detecting targets which pass between the transmitter and receiver, with the bistatic angle, β, near 180 degrees.
- **Multistatic radar** is one in which there are at least three components - for example, one receiver and two transmitters, or two receivers and one transmitter, or multiple receivers and multiple transmitters. It is a generalization of the bistatic radar system, with one or more receivers processing returns from one or more geographically separated transmitters.
- **Passive radar,** this radar system is also known as Passive Coherent Location (PCL) system. Instead of having a dedicated or a non-dedicated transmitter, this receiver uses a third-party transmitter in the environment, like commercial signals and measures the time difference of arrival between the signal arriving directly from the transmitter and the signal arriving via reflection from the object, this allows the bi-static range of the object to be determined.

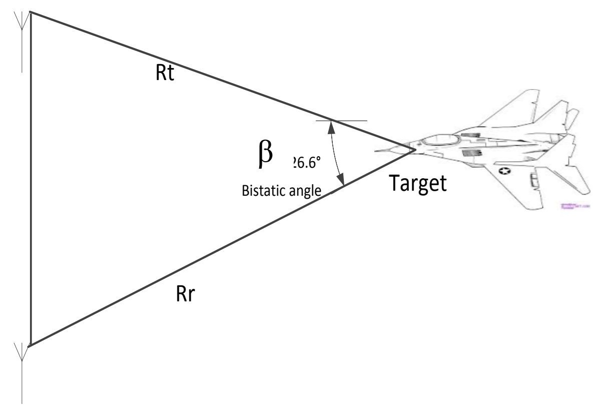

Figure 2 Bistatic angle and Range description

1.4.3 Multistatic Radar Operation Modes

Multistatic radar receivers can operate with their own dedicated, cooperative transmitter or a non-cooperative transmitter that is suitable for the receivers operation. A non-cooperative transmitter is a radar that operates at the receiver frequency and compatible with the receiver phase but it is not designed to operate with the receiver. This type of operation is called "hitchhiker". The first "hitchhiker" was a German radar that uses the enemy radar, the British Chain Home as transmitter for their radar called Klein Heidelberg-Parasite. This radar system was used to detect enemy air attacks [5]. Hitchhikers are also used in the measurement of the ocean roughness. Radar cross section and the brightness temperature of the ocean are sensitive to surface roughness. Ocean surface roughness has been studied by using signals from Global Navigation Satellite System (GNSS) and receivers in aircraft, balloons and satellites [8].

Different conditions and parameters such as: transmitter configuration, receiver and transmitter antenna, the location and distance relative to the target, and antenna pointing direction are critical for the application of the multistatic system. Bistatic radar applications are presented in the following table with the restrictions on transmitter configuration and operation regions.

Bistatic radar Operation regions	Range Relationship (related to target)	Transmitter Configuration		
		Dedicated	Cooperative	Non-Cooperative
Receiver Centered	$R_T >> R_R$	• Silence Penetration • Semi-active homing missile (lock on after launch)	• Short-range air defense • Ground surveillance • Passive situation awareness	• Passive situation awareness
Transmitter Centered	$R_R >> R_T$			• Intelligence data gathering • Missile launch alert
Co-site	$R_t \approx R_r$	• Medium-range air defense • Satellite tracking • Range instrumentation • Semi-active homing missile (lock on before launch) • Intrusion detection		

Table 2 Bistatic radar application according to location and configuration.

1.5 Summary of Following Chapters

Chapter two will present all theoretical background needed for the development of the project, including equations for the antenna design and all theory needed about radar operation for the proper functioning of the receiver. Chapter three will be comprised of all the construction process, the equipment and parts and how the receiver was mounted, the antenna construction, and the solar system implementation. Chapter four will present the characterization and testing of the system and its subsystems. Finally chapter five will present the conclusions, results, recommendations and future work left to the end user. After the last chapter, a user manual will be available for the operation of the system and different images that will help the understanding of the work done.

2. THEORETICAL BACKGROUND

2.1 Radar Theory

Radar has been largely under study since their creation in the 1920s. Even when their original purpose was entirely military, researchers worldwide has found many civil applications such as air traffic control, radar astronomy, marine radars to locate landmarks and other ships; aircraft anti-collision systems; ocean surveillance systems, outer space surveillance; meteorological precipitation monitoring; altimetry and flight control systems; and ground-penetrating radar for geological observations among many more. A very common and simple block diagram of radar is presented below.

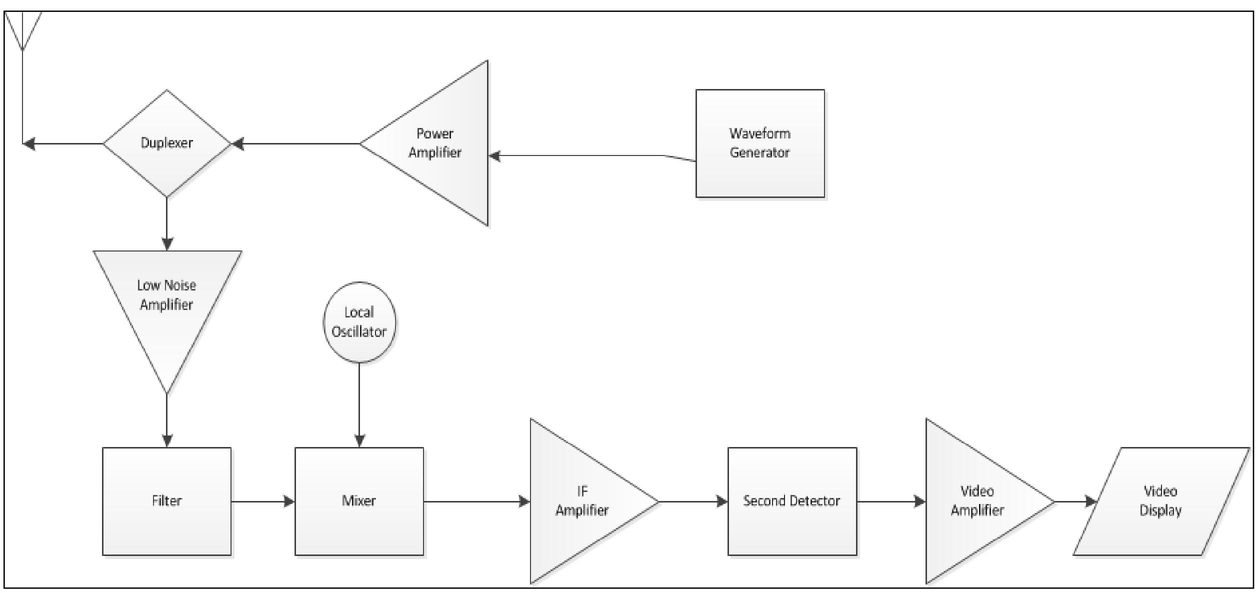

Figure 3 Radar Block Diagram [9]

Figure 3 illustrates the simplest block diagram of a monostatic radar system. It works with a radar wave signal, usually in the form of a train of pulses which is generated by a transmitter and radiated to the air through the antenna. The duplexer allows the system to use a single antenna isolating the transmitter signal from the receiver. The radar signal hits a target or multiple targets and some of the reflected signal, or echoes, are collected by the antenna, detected and interpreted by the receiver system. In the table below the mathematical equations defining important radar parameters and used to understand how the radar works are presented.

Equation Name	Description	Equation
Received Power (Single Target)	Power received by the antenna respect to distance, detected object properties and transmitter radar.	$P_r = \frac{P_t G_t G_r \lambda^2 \sigma_B}{(4\pi)^3 R_T^2 R_R^2}$
Received Power (Distributed Targets)	Power received by the antenna by multiple targets in the volume of the antenna beam.	$P_r = \frac{P_t G_t G_r \lambda^2}{(4\pi)^3} \sum \frac{\sigma_i}{R_{ti}^2 R_{ri}^2}$
Radar Constant	This equation collects all the non-variables in the radar equation to have a singleradar constant K.	$K = \frac{P_T G_T G_R \lambda^2 \sigma_B F_T^2 F_R^2}{(4\pi)^3 \mathbf{K} T_s B_n L_T L_R}$
Radar Cross Section	A measure of how detectable an object is for a radar.	$\sigma = \frac{\pi^5 \lvert K_{ob} \rvert^2 D_i^6}{\lambda^4}$
Unambiguous Range	Maximum range from echoed signal that can be detected after the following pulse is transmitted	$Range = \left(\frac{c}{PRF}\right)$

Table 3 Monostatic set of equations

2.1.1 Noise and Dynamic Range

The effect of noise is vital to RF communications, radars and remote sensing systems because the noise level sets the lower limit of the strength of the signal that can be detected. It is desirable to minimize this noise level to achieve the best performance increasing the sensitivity of the receiver [10]. Some noise sources are:

- Thermal Noise
    - Most basic, caused by thermal vibrations of bound charges.

- Shot Noise
  - Fluctuations of charge carriers in electron tube or solid state devices.
- Plasma Noise
  - Caused by random motion of charges in an ionized gas.
- Quantum Noise
  - Results from quantized nature of charge carriers and photons, often insignificant relative to the others.

2.1.1.1 Noise Figure

A noisy RF component can be characterized by an equivalent noise figure [10]. Noise figure (F) is a measure of degradation in the signal-to-noise ratio between the input and the output of the system. The signal–to-noise ratio is the ratio given by the desired signal over the undesired circuit noise. The noise figure can also be written as: [10]

$$F = 1 + \frac{T_e}{T_0}$$

Where,

$F = Noise\ figure$ $\quad$ $T = Noise\ Temperature$

$T_0 = Room\ temperature$ $\quad$ $G = Gain$

2.1.1.2 Cascade Noise Figure

In a typical microwave system the input signal travels through a cascade of different components, each of them contribute to the system noise figure. The cascaded system noise figure equation is [10]:

$$F_{cas} = F_1 + \frac{F_2 - 1}{G_1} + \cdots + \frac{F_n - 1}{G_{n-1}}$$

It is noticeable from the equation that the first element is the most significant contributor to the system noise figure.

2.1.1.3 Dynamic Range

Non component can be considered completely linear. The linear region of an active component is where the output is directly proportional to the input and deterministic, which means that is predictable from the input for an unlimited range of input/output signal levels. This characteristic is true for a specific region called the Dynamic Range. The dynamic range is a well known radar parameter which is different for every receiver system. It is defined as the range of signal levels where the receiver's input and output posses a linear relationship. In a radar system, the receiver's noise floor determines the lower bound on sensitivity known as minimum detectable signal (MDS). On the other hand, the upper bound is set by the receiver's saturation point also known as its 1dB compression point. That is the input power for which the output is 1 dB below that of the ideal amplifier gain [11]. With this information the power return from objects that can be detected in the linear region of the particular receiver are defined. An example of the dynamic range plot is presented in Figure 4.

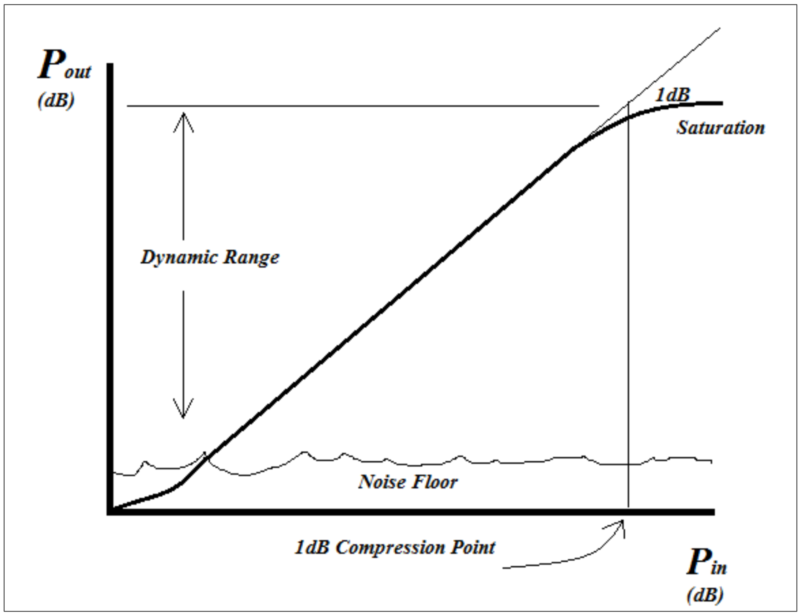

Figure 4 Receiver dynamic range example

2.1.2 Bistatic Radar

The Bistatic or multistatic radar system uses different antennas for receiving and transmitting, as a result there has to be one or more antennas for either the transmitter or the receiver, for example, one transmitter with multiple receivers, or vice-versa, or there is also the case with multiple transmitters and receivers.

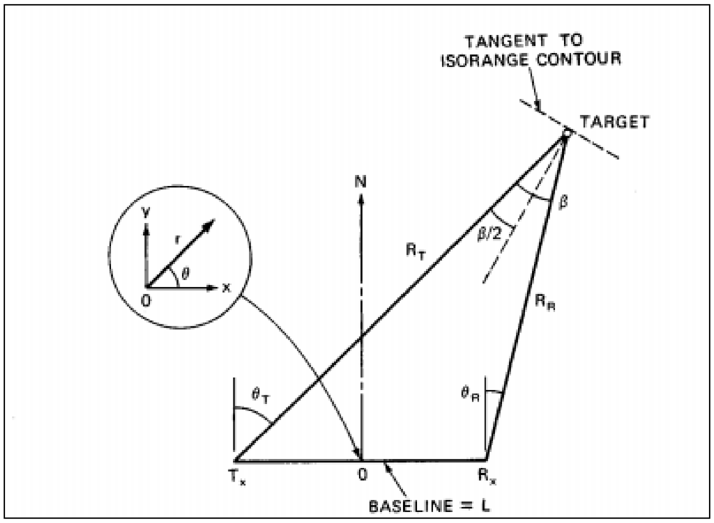

Figure 5 Bistatic radar geometry

Basically, monostatic radar equations are a special case of the bistatic configurations, since the terms for the bistatic equations are presented in a more general form. The differences between the two are a few parameters, specifically parameters that take into consideration the signal incident angle and the target distance respect to the antennas. Depending on the author, there are slight variations in the name given to the different variables; in this case all notations are taken from the *Bistatic Radar by Nicholas J. Willis [2005].* A set of equations needed for the correct understanding of the bistatic radar system are shown in Table 4.

Equation Name	Description	Equation
Received Power	Power received by the antenna respecting distance, detected object properties and transmitter radar.	$P_r = \frac{P_t G_t G_r \lambda^2 \sigma_B}{(4\pi)^3 R_T^2 R_R^2}$
Radar Constant	This equation collects all the non-variables in the radar equation to have a single value to apply *K*.	$K = \frac{P_T G_T G_R \lambda^2 \sigma_B F_T^2 F_R^2}{(4\pi)^3 \mathbf{K} T_s B_n L_T L_R}$
Bistatic Range	This equation shows the maximum distance that an object can be detected by the bistatic system.	$(R_T R_R)_{max} = \left(\frac{P_T G_T G_R \lambda^2 \sigma_B F_T^2 F_R^2}{(4\pi)^3 \mathbf{K} T_s B_n \left({}^{S}/_{N} \right)_{min} L_T L_R} \right)^{\frac{1}{2}}$
Signal to Noise Ratio	Bistatic range equation solved in terms of the signal to noise power ratio.	${}^{S}/_{N} = \frac{K}{R_T^2 R_R^2}$

Table 4 Bistatic radar equation

Where:

$R_T = Range\ Transmitter\ antenna\ to\ target$

$R_R = Range\ Receiver\ antenna\ to\ target$

$P_T = Transmitter\ Power$

$G_T = Transmit\ Antenna\ Gain$

$G_R = Receive\ Antenna\ Gain$

$\sigma_B = Bistatic\ Radar\ Cross\ Section$

$F_T = Pattern\ propagation\ factor\ for\ transmitter\ to\ target\ path$

$F_R =\ Pattern\ propagation\ factor\ for\ target\ to\ receiver\ path$

$D = Diamater\ of\ the\ target$

$PRF = Pulse\ Repetition\ Frecuency$

$\beta = bistatic\ angle$

$T_s = Receive\ system\ noise\ temperature$

$B_n = noise\ Bandwidth\ of\ receiver's\ filter$

$L_T = Transmit\ Losses$

$L_R = receive\ Losses$

$({}^{S}/_{N})_{min} = signal\ to\ noise\ ratio$

K $= Boltzmann's\ constant$

$\lambda = wavelength$

K = *bistatic radar constant*

$K_{ob} = Complex\ Dialectric\ factor\ the\ object$

$c = light\ velocity$

$\frac{\beta}{2} = bistatic\ bisector$

As seen in Figure 5, the target, the transmitter and receiver antennas locations always form a triangle. The beta angle is known as the bistatic angle, this angle is limited to be very close to 0 degrees or very close to 180. If the bistatic angle, β, is zero the system is called pseudo-monostatic radar and at 180 the target is blocking the signal. The baseline (L) is very important in the target location detection and in the *SNR* (Signal to Noise Ratio) calculation. The SNR in the bistatic radar is given by the Cassini Ovals, explained below.

2.1.3 Bistatic radar Synchronization

For bistatic radar systems, the synchronization technology is one of the most important key techniques. For ground based bistatic radar with moderate bandwidth, time and frequency synchronization is easily obtained by a global positioning system (GPS), which provides a stable pulse per second signal (PPS) [12]. According to GPS developers two distant units seeing the same satellites may have a standard deviation as low as 15 ns. Therefore the use of disciplined GPS oscillators maintains two separated sites synchronized or coherent. Even when there is only one synchronization signal source, there are two different synchronizations needed, they are Time Synchronization (TS), and Frequency and Phase Synchronization (FPS) [13].

- Time Synchronization

  - Is required for range measurements. A typical requirement for time synchronization is about a tenth of the transmitter pulse width. This time synchronization can be achieved in many ways; time synchronization signal can be sent by optical fiber or coaxial cable, a microwave link if there is line of sight, or by satellite communication if both the above conditions are not available [13]. The 1PPS (one pulse per signal) triggers the start of the transmitter and the receiver local oscillator, it also provides the time in Universal Time Code (UTC) to be stored by the data acquisition system [12].

- Frequency and Phase Synchronization

  - Frequency and phase synchronization is essential for the pulse compression and Doppler capability of the system. In monostatic systems a sample of the transmitted signal is taken to determine the original phase in order to determine the Doppler Effect. In bistatic systems transmitter sample is impossible to take if the transmitter and receiver are far apart, that's why this synchronization is accomplished by the use of match GPS disciplined local oscillators [12].

2.1.4 Bistatic Doppler

The frequency shift derived from the Doppler Effect, resulting from motion of the target, the transmitter, or the receiver is different from what is observed in monostatic radar. In monostatic the Doppler shift, f_d is found from the velocity component of the target moving towards or away from the antenna. The bistatic Doppler shift is generally described by the contribution of range rates in both ranges from the receiver and transmitter as [14]:

$$f_d = \frac{1}{\lambda}\left(\frac{dR_t}{dt} + \frac{dR_r}{dt}\right)$$

Range rates can be expressed by the target velocity V in the bistatic plane, bistatic bisector (Figure 5), and angle δ [1]. δ is the angle formed by the velocity vector, v_M, of target movement and the bistatic bisector. Then the frequency shift resulting expression is:

$$f_d = 2\frac{v_M}{\lambda}\cos\delta\cos\frac{\beta}{2}$$

2.1.5 I/Q Signals [29]

Radar signals are classified as “narrow band signals”. Because of that the Fourier transform is non-negligible only in a finite band of frequencies. This signal can be represented as

$$x(t) = a(t)\cos[2\pi f_0 t + \alpha(t)]$$

where f_0 is the carrier frequency, the functions $a(t)$ and $\alpha(t)$ represents the amplitude and phase modulation of the signal respectively. This equation can be written as;

$$x(t) = a(t)\cos\alpha(t)\cos 2\pi f_0 t - \alpha(t)\sin\alpha(t)\sin 2\pi f_0 t$$

$$= I(t)\cos 2\pi f_0 t - Q(t)\sin 2\pi f_0 t$$

Where $I(t)$ and $Q(t)$ are the in-phase and quadrature phase components of the modulation, respectively. Then the complex signal $s(t)$ corresponding to the real signal $x(t)$ is defined as;

$$s(t) = [I(t) + jQ(t)]e^{j2\pi f_0 t}$$

where $I(t) + jQ(t) = U(t)$ that is the complex envelope of the signal.

In order for the receiver to be able to determine the velocity of an object I/Q mixers and demodulator are needed. An I/Q mixer is a mixer that shift by 90 degree the input signals and an I/Q demodulator is a device whose function is to produce the in-phase (I) and the quadrature (Q) components of the complex envelope explained before.

2.1.6 Cassini Ovals

The formal definition of an oval of Cassini is the locus of the vertex of a triangle when the product of the sides adjacent to the vertex is constant and the length of the opposite side is fixed [15]. A simple definition can be; a curve defined as the set (or locus) of points in the plane such that the product of the distances to two fixed points is constant [16]. In a bistatic radar system these ovals are defined as the SNR contours where the range product, $(R_T R_R)$, remains constant. In order to obtain such ovals, the bistatic range equation is solved for the SNR. Ovals in Figure 6 are contours of constant SNR on any bistatic plane, assuming that an adequate LOS (Line-of-sight) exists on the transmitter-to-target path and the receiver-to-target path, also that radar cross section and noise figure are independent of radius and angle (which is usually not the case). The lowest SNR is in the outer contours and increases while getting closer to the antennas.

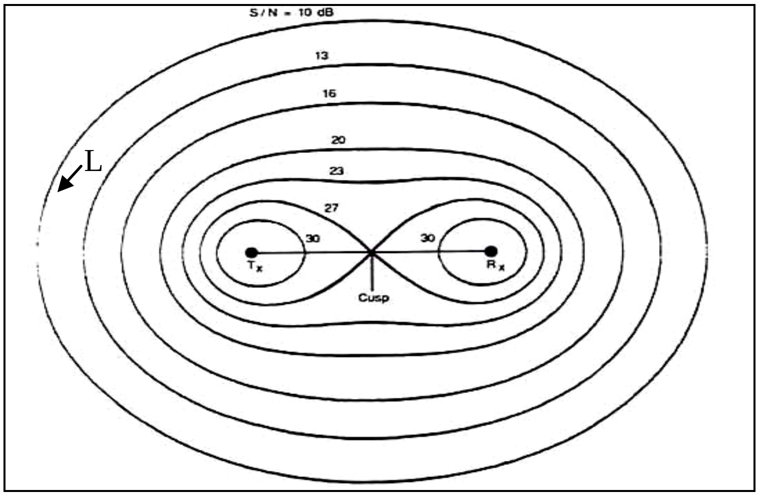

Figure 6 Cassini oval example

Ovals of Cassini define three distinct operating regions for a bistatic radar:

- Receiver-centered region
    - Small oval around the receiver in Figure 6.
- Transmitter-centered region
    - Small oval around the transmitter in Figure 6.
- Cosite Region, receiver-transmitted-centered region
    - Any other oval in Figure 6.

Examples of applications for every operating region are available in Table 2

2.1.7 Bistatic Radar Cross Section

Bistatic radar cross section (RCS) is a measure similar to the monostatic RCS related to the energy scattered from the target in the direction of the receiver. Bistatic RCS is more complex than the monostatic because is a function of aspect angle and bistatic angle. The Crispin and Siegel monostatic-bistatic equivalence theorem says that for vanishingly small wavelengths, the bistatic RCS of a sufficiently smooth, perfectly conducting target is equal to the monostatic RCS. Sufficiently smooth targets typically include spheres, elliptical cylinders, cones, and gives (a roundly tapered end of a two-dimensional or three-dimensional object.), Three regions of bistatic RCS are of interest: pseudo-monostatic, bistatic, and forward-scatter (sometimes called near-forward-scatter) each region is defined by the bistatic angle [1].

1. Pseudo monostatic
    a. For $\beta < 20^0$, for $\beta < 5^0$, the RCS of a target is equal to the monostatic RCS.
2. Bistatic
    a. For $20^0 < \beta < 140^0$
3. Forward scatter
    a. For $\beta > 140^0$

2.2 Antenna Theory

Antenna is a critical device that is used to transfer guided electromagnetic waves (signals) to radiated EM waves in an unbounded medium (usually air) [17]. There are many antenna types: wire antennas, reflector antennas, aperture antennas, etc. Every single antenna is designed for specific applications and will have benefit and cons. In this project an S-band Dual-Pol microstrip antenna was used because of its low-cost and availability of machinery for construction in the lab.

2.2.1 Microstrip Antennas

Microstrip antennas are currently one of the most popular because it presents attractive features such as low profile, light weight, small volume and low production cost. In addition, the benefit of integrating the feed network on the same substrate presents a great advantage [18]. The idea of the microstrip antenna dates back to the 1950's, but it was not until the 1970's that serious attention was given to this particular element. As seen in Figure 7 a microstrip antenna is simply a metallic patch printed on a thin, grounded, dielectric substrate. Researchers around the globe have developed dozens of variations to the original microstrip antenna design, variations in shape, feeding techniques, array geometries and substrate configurations [19]. Some disadvantages of the microstrip antenna configurations include narrow bandwidth, spurious feed radiation, poor polarization purity, and limited power handling. Much of the research work in microstrip antennas has thus gone into trying to overcome these problems, in order to satisfy increasingly rigorous systems requirements. This effort has produced the development of novel microstrip antenna configurations, as well as accurate and versatile analytical models for the understanding of the inherent limitations of microstrip antennas, as well as for their design and optimization [20].

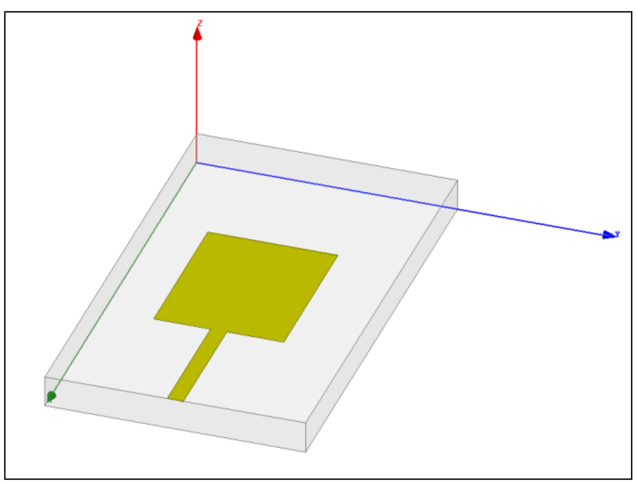

Figure 7 Microstrip Antenna

Table 5 presents the basic equations needed to start a simulation design of a microstrip patch antenna and the feed network [17].

Square Patch Antenna Equations		
Square patch antenna width	$$W = \frac{c}{2f_0\sqrt{\frac{(\varepsilon_r)}{2}}}$$	
Antenna Length	$$L_{reff} = \frac{c}{2f_0\sqrt{\varepsilon_{reff}}}$$	
Feed Network Lines		
Effective dielectric constant	$$\varepsilon_{reff} = \frac{\varepsilon_r + 1}{2} + \frac{\varepsilon_r - 1}{2}\left[1 + 12\frac{h}{W}\right]^{-\frac{1}{2}}$$	
Physical line length	$$\theta^o = \sqrt{\varepsilon_{reff}}\left(\frac{2\pi f_0}{c}\right)l$$	
Line width	For $w/h \leq 1$	$$Z_{desired} = \frac{60}{\sqrt{\varepsilon_{eff}}}ln\left(\frac{8h}{w} + \frac{w}{4h}\right)$$
	For $w/h \geq 1$	$$Z_{desired} = \frac{120\pi}{\sqrt{\varepsilon_{eff}}\left[{}^{w}/_{h} + 1.393 + .667ln\left({}^{w}/_{h} + 1.444\right)\right]}$$

Table 5 Microstrip antenna patch design equations

2.2.2 Antenna Gain and Radiation Pattern

The antenna radiation pattern is a display of the radiation properties of an antenna as a function of the spherical coordinates (θ,φ) [21]. Figure 8 illustrates an example of how an antenna radiation pattern looks like for a dipole antenna increasing the distance from the ground.

An antenna being a passive element it does not add gain to the power input. Therefore the term, antenna gain describes how much power is transmitted in the direction of peak radiation to that of an isotropic source. There are 5 basic methods to change the overall antenna radiation pattern [22]:

- By the geometrical configuration of the overall array.
- By the displacement of the radiating elements
- The excitation amplitude of individual elements
- The excitation phase of each element
- The relative pattern of each element

In Figure 8 it is observed in pattern D the presence of nulls, as the distance to ground increases more nulls are evident. Nulls are in directions where the antenna do not radiates energy. By the principle of conservation of energy, energy cannot be created or destroyed, the energy focuses into the directions that is radiating and form a main radiation (or side radiation) lobes. These lobes have more energy in the particular direction than before and that is how gain is increased [23].

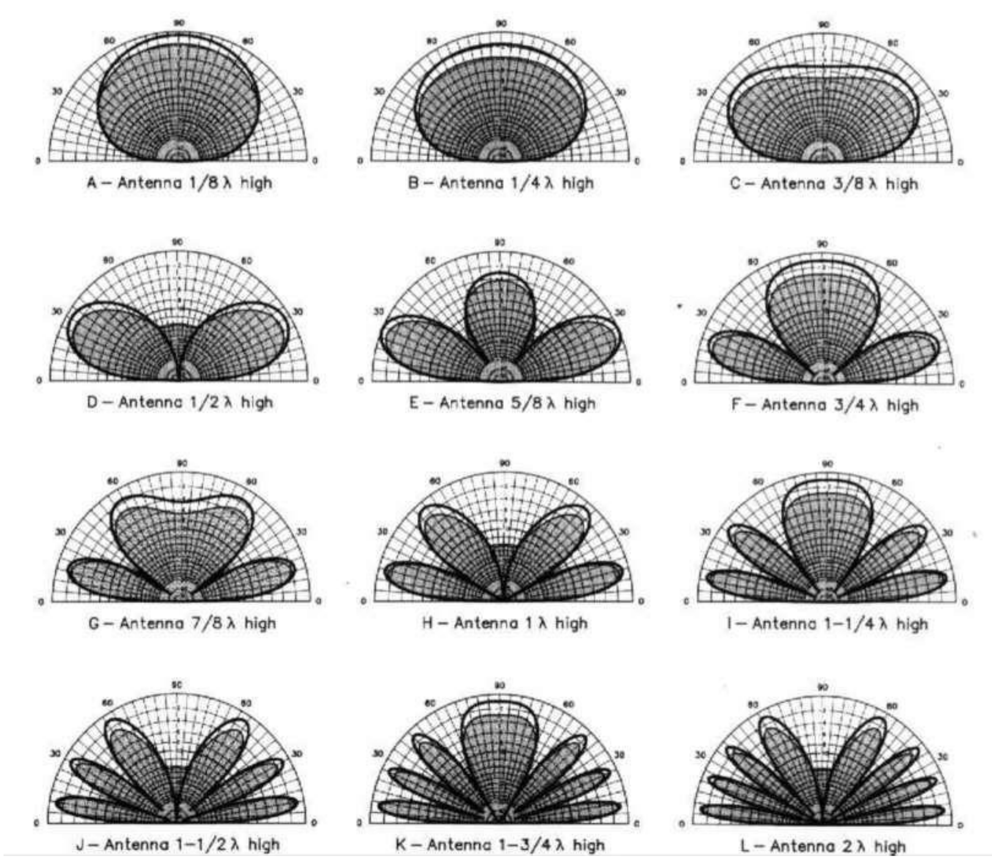

Figure 8 Antenna radiation patterns [24]

2.2.3 Antenna Polarization

Polarization of a radiated wave is defined as the property of an EM (electromagnetic) wave describing the time-varying direction and relative magnitude of the electric field vector; specifically, the figure traced as a function of time by the point of the vector at a fixed point in space, and the sense it is traced [25]. In other words, polarization is the curve traced by the end point of the arrow (E-vector) representing the instantaneous electric field. The field must be observed along the propagation direction [25]. Antenna polarization is then the curve traced by the radiation pattern. An image with two different types of polarization signals is presented in Figure 9.

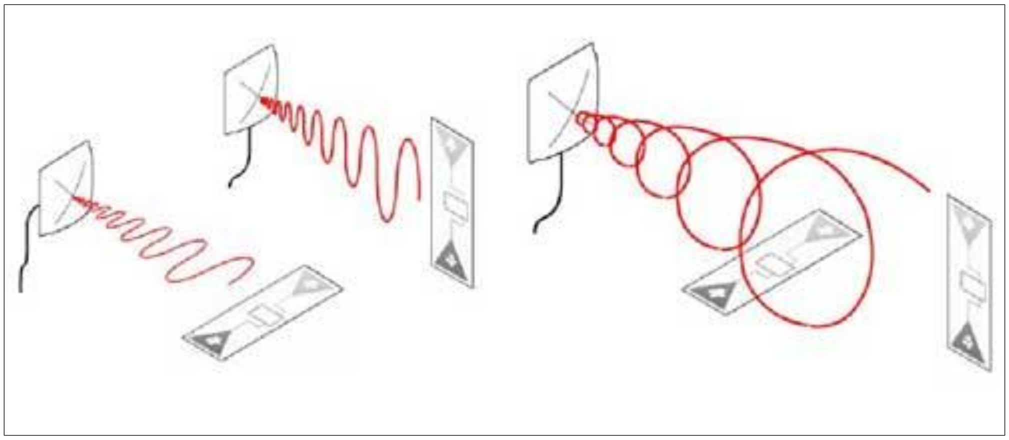

Figure 9 Illustration of linear and circular polarization [28]

There are three kinds of polarization: linear, circular, and elliptical polarization [25].

- Linear polarization
  - An antenna is linearly polarized if the end point of the electric field vector of the antenna radiation pattern is always oriented along a straight line at every time.
- Circular polarization
  - An antenna is circularly polarized if the end point of the electric field vector of the antenna radiation pattern traces a circle as a function of time.
- Elliptical polarization
  - An antenna is elliptically polarized at if the end point of the electric field vector of the antenna radiation pattern traces an elliptical locus as a function of time. Circular and linear polarization are considered special cases of elliptical polarization.

Dual polarization antenna refers to an antenna that possesses two different polarization lines. A typical example is when an antenna is linearly polarized in two different directions such as horizontal and vertical.

2.2.4 Antenna Array

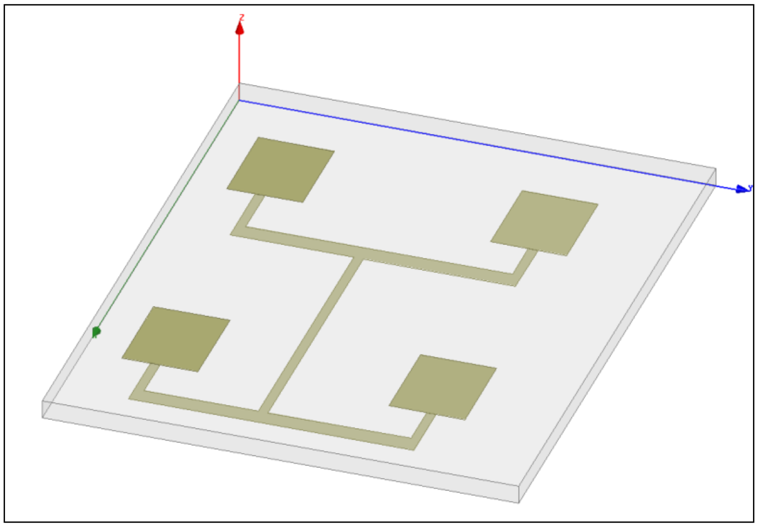

Figure 10 Antenna Array

Many applications require radiation with high gain characteristics, which may not be achievable by a single element. It may, however, be possible that an aggregate of radiating elements in an electrical and geometrical arrangement (an array) will result in the desired radiation characteristics. The arrangement of the array may be such that the radiation from the elements adds up to give a radiation maximum in a particular direction, minimum in others, or as desired. [25] An array of identical elements with identical magnitude and each with a progressive phase is referred as a uniform array. Adding identical elements to the antenna it is seen that the total field is equal to the original field multiplied by a factor, known as the array factor. This array factor can be written as:

$$AF = \sum_{n=1}^{N} e^{j(n-1)\Psi} \quad \text{Where:}$$

$$\Psi = kd\cos(\theta) + \beta$$

3 System Design

3.1 Purpose

The main goal of the project is to modify a low cost S-Band radar receiver already developed in CSU. This original prototype met all the required specifications, and during the second phase of the project an approach to minimize cost was adopted by relaxing some of the specifications. The receiver has to be easy to deploy and replicate. In order to achieve the low-cost requirement the most expensive components of the already developed receiver has been replaced.

In order to achieve the low-cost goal, it was determined to replace the DAQ system, the antenna, the GPS reference system, the enclosing device and the portable stand from the original version. The main specifications are summarized as;

- Receiver to operate at 2.725 GHz.
- Dual-Pol and Doppler capability.
- Solar powered.

3.2 RF Operation

The RF block diagram (see Figure 11), is a visual representation that shows how the receiver works in terms of the received RF or microwave signal. When a signal is received by the antenna is rapidly amplified by the low noise amplifiers (LNAs). The first component is a low noise amplifier, which basically set the noise floor of the receiver. After amplified, the signal gets filtered, this is to get rid of any undesirable frequency signal, in this case an 80 MHz bandwidth band pass filter is centered at 2.725GHz. After filtered, the signal is mixed with a local oscillator signal to obtain the intermediate frequency signal (IF). This IF signal is a low frequency, easier to process signal for the data acquisition system. The local oscillator is a phase lock dielectric resonator oscillator (PLDRO), at 2.700GHz. The local oscillator signal is disciplined by a GPS reference system (see section 2.1.3). The GPS reference system for this project is a Quartzlock E8-X OEM (see Appendix C). This GPS reference have two outputs 1PPS and a 10MHz sine that are used to give clock to the DAQ and to lock the PLDRO respectively. This local oscillator signal is mixed with the received signal at the I/Q mixers. The I/Q mixers consist of ordinary mixers that multiplies the signal carrying the information with the local oscillator signal, with one of them 90^0 shifted. This is very important for the determination of the Doppler effect since those calculations are done with the I/Q signals. The output signals of the mixers are the inputs for the data acquisition system. Doppler capability demonstration is not part of this project. The mixers and data acquisition system are ready and capable of Doppler data manipulation for future applications. Since the system is a dual polarization receiver, the process is repeated for each of the polarizations, as Figure 11 shows the V and H channel.

Figure 11 Receiver Block Diagram

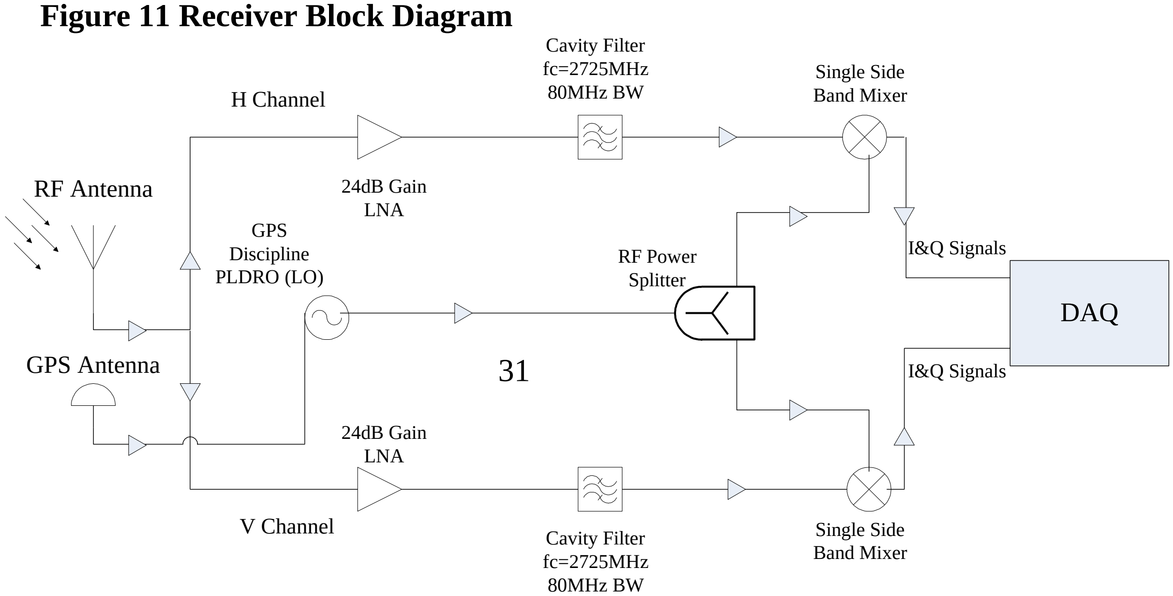

3.3 Data Acquisition System

One of the modifications made to the original design is the data acquisition card. The data acquisition board used in the previous version is the eDAQ1b from Ridgeline Instruments. The eDAQ1b, as described by their developers, is a small form factor, single board, dual-channel digital receiver governed by an embedded microcontroller running a full-size Linux operating system. The eDAQ1b control interface and digital receiver data output share a single 1GB Ethernet port, avoiding the need for a network switch. Some of eDAQ1b's features are a programmable gain analog front end, sampling speed in excess of 230 MSps, high-resolution tunable down-conversion frequency for automatic frequency control applications, external or on-board reference clock options, miscellaneous I/O channels [26]. The eDAQ1b is a state of the art data acquisition card that cost around $23,000. In order to make a low cost receiver it was agreed to look for a DAQ card that matches the eDAQ1b performance only in the real time data acquisition. Various commercial systems where considered for this project and they are presented in Table 6.

Data Acquisition Card	Characteristics	Price
	24-bit resolution ADCs with 110 dB dynamic range	

NI PCI-4474	4 simultaneously sampled analog inputs at up to 102.4 kS/s ±10 V input range or ±31 V with SMB-120 cable Software-configurable AC/DC coupling and IEPE conditioning	$2,782
NI PCI-4461	24-bit resolution ADCs and DACs with 118 dB dynamic range 6 gain settings for input ranges from ±316 mV to 42.4 V 2 simultaneously sampled analog inputs at up to 204.8 kS/s 2 simultaneously updated analog outputs at up to 204.8 kS/s Software-configurable AC/DC coupling and IEPE conditioning Variable antialiasing and anti-imaging filters and TEDS support	$4,119
Adlink PCI-9820	14- bit A/D resolution Up to 60MS/s 2-CH single-ended bipolar inputs 512 MB onboard RAM	$2,717
Adlink PCI-9812	4 CH- 20MS/s simultaneous 4 CH with 4 independent Analog to digital converter 12-bit A/D Programmable sampling rate 512 MB onboard RAM	$2,417

Table 6 Studied data acquisition cards

After carefully considering every single card, it was determined that the best choice is the NI PCI-4461, but it is still too expensive in order to keep the requirement of a low cost receiver. The second best choice was the Adlink PCI-9820 but the item was unavailable and the estimated time for arrival was too long (8 to 12 weeks). The NI PCI-4474 had all characteristics needed but lack the analog input ports. The selection made, due limited choices, was the Adlink

PCI-9812. The PCI-9812 was the selected card for the first radar receiver modified in UPRM. Adlink still sells the PCI-9812 card but it operates under an outdated OS system that is why the computer runs in an old version of Linux kernel.

The DAQ system is composed of the Adlink PCI-9812 digitizer with I/Q capabilities (see section 2.1.5) connected to a low power computer. This computer will be used to access the DAQ remotely and to storage the acquired data. Computer possesses;

- a 32 bits quad core 1.8GHz processor,
- 4GB RAM
- 500GB Hard Drive
- Ubuntu 10.4 (for compatibility with the DAQ drivers)

The PCI-9812 possesses 512MB of processing RAM on card and during installation there is an option to reserve part of the computer RAM for the card. This allows the card to be suitable for real time data acquisition. The computer has two networks ports; this is for an external user to directly connect to it while the computer is connected to the network at the same time. As seen in Figure 12 the PCI-9812 inputs are BNC ports. The PCI-9812 card is connected to the computer through the PCI slot giving it 33MHz connection, which means a 133MB/s velocity. This velocity is obtained by simply multiplying the connection frequency 33Mhz by the computer system bytes, in this case the computer is a 32 bits system or 4 bytes.

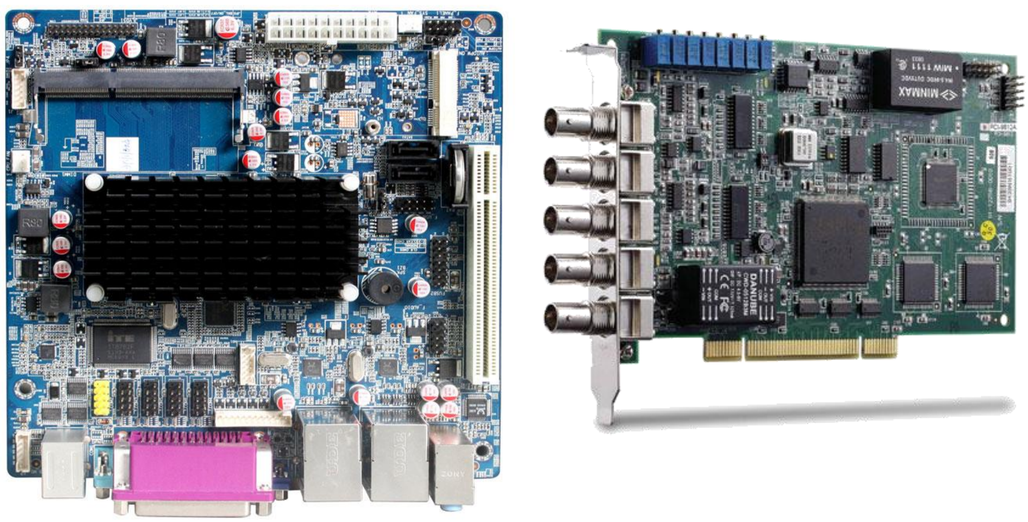

Figure 12 Computer and Data Acquisition Board

3.4 Solar Circuit

Solar power will be used to activate the low-power receiver. Solar circuit calculation takes into account equipment power consumption, the daily power consumption, and solar radiation in the location, among other things [27]. An Excel® spreadsheet has been prepared where the parameters are entered and the program outputs are the solar equipment needed for the project. Excel spreadsheet are presented in Appendix A with all the input data considered.

Power consumption in the circuit is distributed as following:

- GPS Reference
- PLDRO
- LNA

≈ 7 Watts

- Computer ≈ 25 Watts

The total power consumption for the receiver is below 40 Watts. All DC powered components operate at 12V so the battery and solar panel are 12DC Voltage. After calculations, one solar panel of 50W and a 20Amp/h battery is enough to power the whole receiver. In Puerto Rico this represents that the system can operates with a battery fully charge for 5 hours daily for two days without need of recharging.

3.5 Antenna

For this project, the antenna selected will be a microstrip patch array with the typical bandwidth and the maximum gain possible,

Desired antenna requirements are:

- 2.725GHz operation frequency
- Dual Polarization (Horizontal and Vertical)
- 12dBi Gain minimum
- -30dB port isolation

3.5.1 Simulation Software

Designer® or name of company or web is a software based on Method of Moments and use full wave electromagnetic functions for planar analysis based on Maxwell's equations. It computes the input impedance and radiation characteristics for arbitrary shape antennas. Designer can produce three types of meshes, an adaptive mesh, which is a more accurate mesh and more time and memory consuming, an edge mesh, and a simple mesh, which is the least accurate of the three options. The mesh is simply made of triangles and rectangles created over the structure under test to calculate the E fields in each and every one of them. How the structure is meshed depends on the adaptive or static selection.

The static mesh (normal or edge mesh) depends on the meshing frequency; the adaptive mesh will be denser until a particular response converges. If both meshes provide an accurate response, the adaptive one would most likely be less dense than the static one. As the structure grows more complex, the adaptive mesh estimation becomes more time consuming than the static one. Discontinuities and overlapping in the drawing will cause the mesh to have more polygons in these areas causing more time and memory consuming simulation. Static mesh, the mesh used for the antenna simulations, has a trade off, the higher the frequency the more precise the final mesh will be, but more time consuming creating a mesh at a frequency lower than the resonant frequency will produce inaccurate results.

3.5.2 Antenna Design

In order to determine patch antenna dimensions and impedance, a single patch antenna is designed first. This antenna element was constructed and the material used was the Rogers R3003. In order to make the calculations the following data is needed:

- Relative permittivity $\varepsilon_r = 3.0$
- f=2.725GHz
- Thickness h = 1.52mm
- λ=.11m

With the above values inserted in equations of Table 5 the antenna dimensions results are shown in Table 7:

Square Patch Antenna Equations	
Square patch antenna width	$W = 45mm$
Antenna Length	$L_{reff} = 37.3mm$
Feed Network Lines	
Effective dielectric constant	$\varepsilon_{reff} = 2.18$

Table 7 Antenna Calculated Dimensions

Antenna resonance frequency is primarily given by the length of the antenna so the square patch was designed using L_{reff} as the original length and width. Optimization was needed since the antenna did not resonate at the desired frequency. After the optimization, dimension results to be 30.7mm. This is almost 7mm smaller compared to the calculated one.

The return loss or $|S_{11}|$dB is a parameter that shows how well matched is a device, in this case the antenna match. For this project the goal is to achieve at least a return loss of 10dB. The return loss for the single patch antenna is presented in Figure 13.

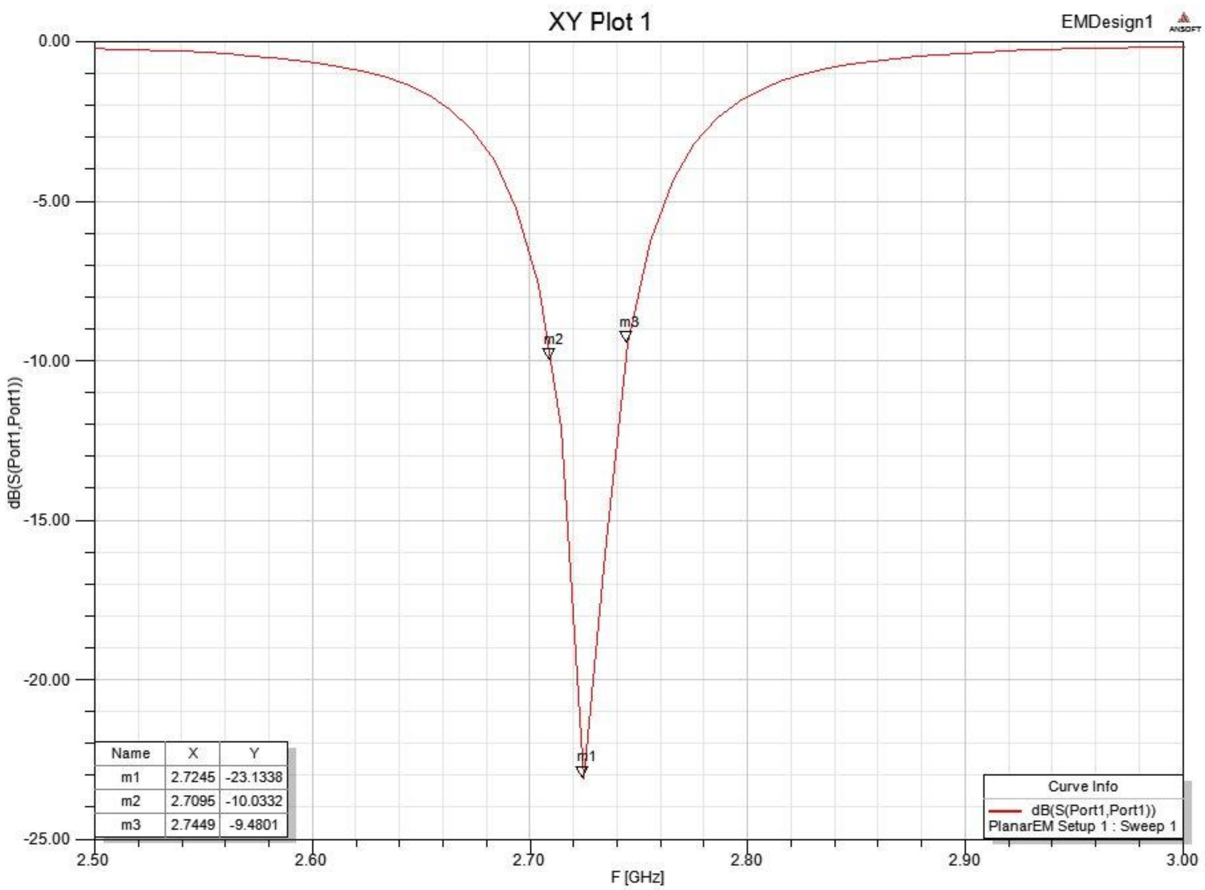

Figure 13 S11 or return loss for a single square patch

To determine how many elements will have the array, the gain of the single patch antenna needs to be calculated. The antenna gain is 6 dBi as seen in the radiation pattern plot from Figure 14. This meant that to obtain the minimum desired gain of 12dBi an array of four patches was needed to achieve the goal.

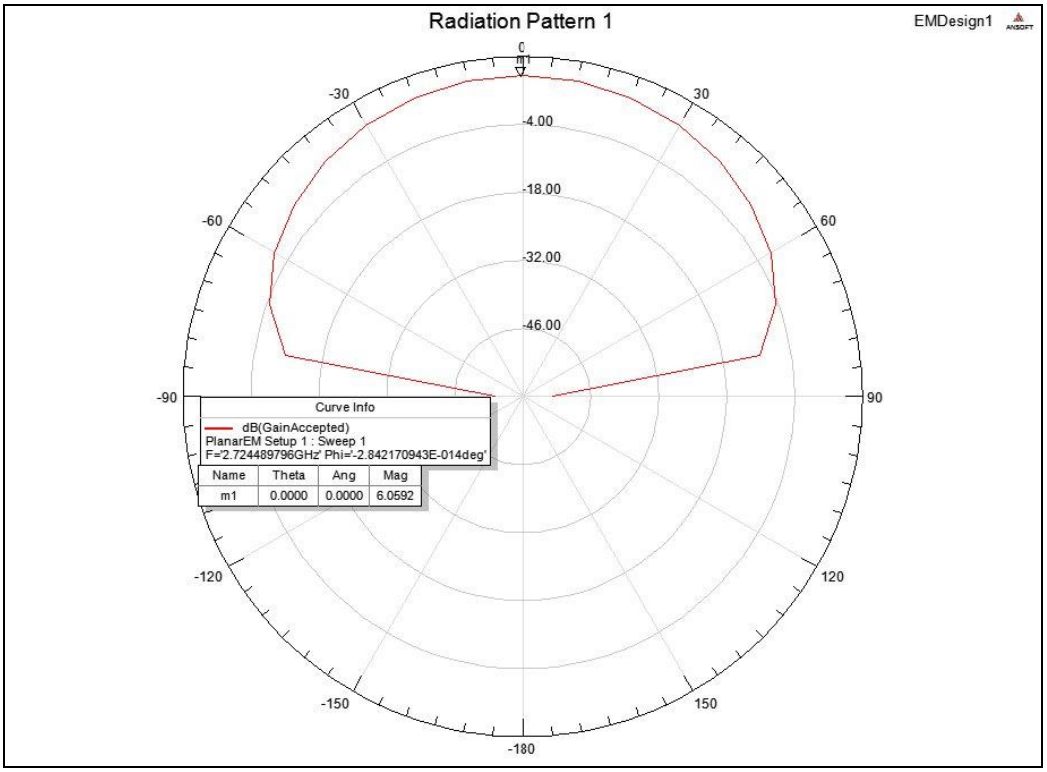

Figure 14 Single patch gain

The array consists of four square patches separated half wavelength from each other. The quarter wavelength transformers in Figure 15 are made in order to make the feed lines thicker, due to limitations of the available milling machine. In Figure 15 it is presented that the antennas placed on the right are fed by the right side while the antennas on the left by their left sides. The same occurs with the upper and lower antennas that are fed by the upper side and lower side respectively. This causes a 90 degrees phase shift in the radiation pattern that is corrected by shifting 90 degrees the feeder location in the transmission line.

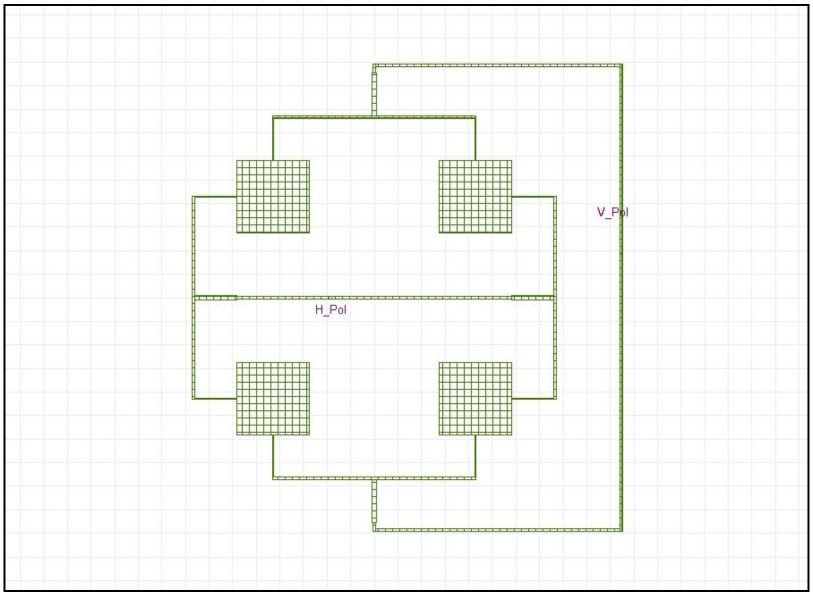

Figure 15 Selected antenna array configuration

Figure 16 presents the return loss of the complete antenna with the complete feed network. The return loss for the horizontal polarization is -15dB and -15.75 for the vertical polarization.

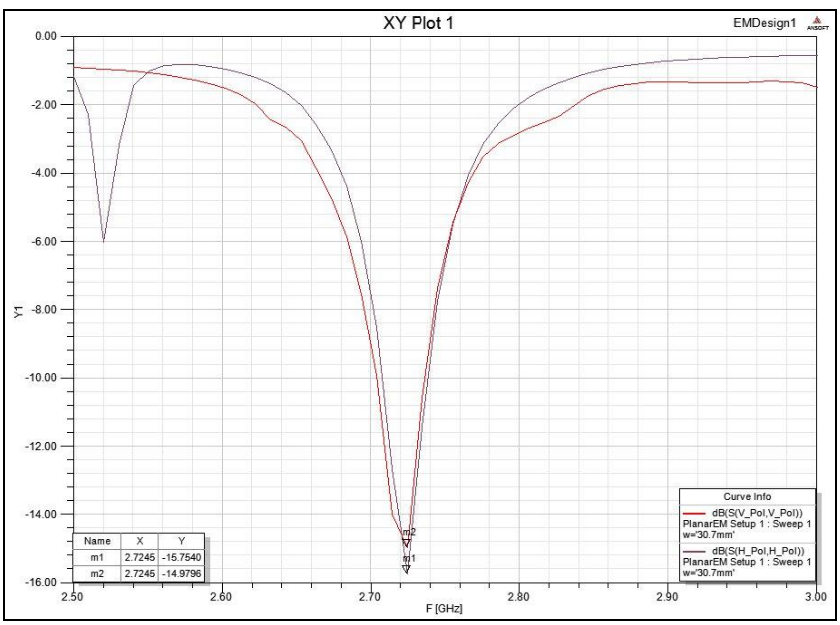

Figure 16 Return loss for the complete array

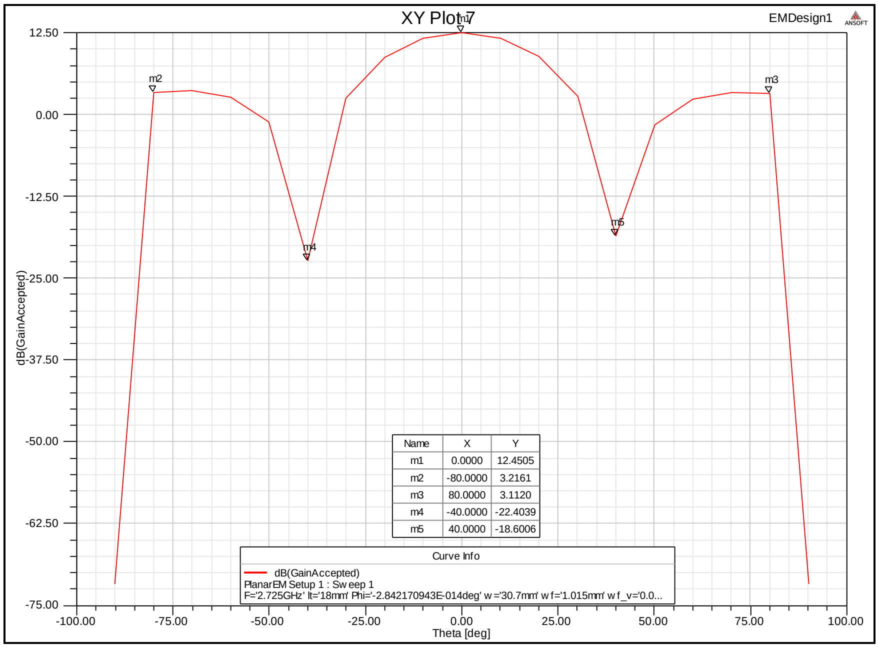

Figure 17 Complete antenna array gain

Figure 17 shows the gain of the complete array. Section 2.2.2 explains the nulls and lobes observed when adding elements to the array. Figure 18 is a plot that shows how well isolated are the ports to each other. Isolation between the H and V channel is considered good in this case since the port isolation or S_{21} is higher than 30 dB.

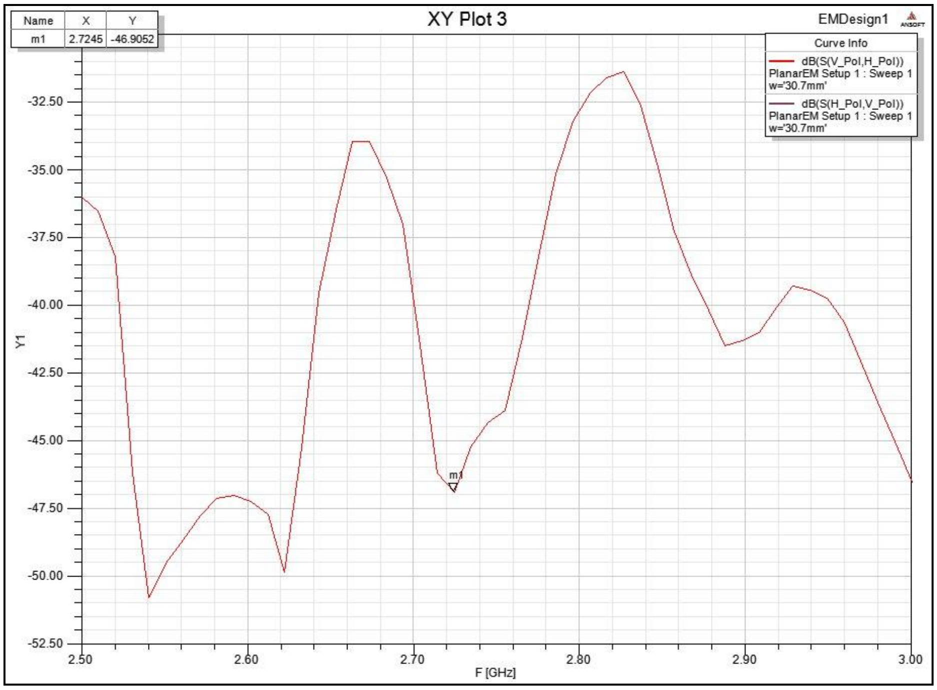

Figure 18 S21 or port isolation for the complete antenna array

4 Test and Construction

4.1 Components

Table 8 presents all the selected components with their price and the price difference compared to the previous prototype. Components which are made in the university are described as “In Home” under the distributor column.

Components	**CSU Model**		**UPRM Model**		**Cost Difference (CSU-UPRM)**
	Distributor	**Cost**	**Distributor**	**Cost**	
RF Circuit Components					
Amplifiers	CIAO	$850.00	CIAO	$850.00	$0.00
Filters	LORCH	$505.00	LORCH	$505.00	$0.00
Freq. Mixers	MITEQ	$590.00	MITEQ	$590.00	$0.00
RF Power Splitter	MiniCircuit	$24.95	MiniCircuit	$24.95	$0.00
PLDRO	MITEQ	$1020.00	AtlanticMicrowave	$1630.00	-$610.00
Antenna					
RF Antenna	Seavey Engineering	$9,800.00	In Home	$87.00	$9,713.00
Antenna Holder	Machine Shop	$124.84	K-Mart (weather proof protector)	$35.00	$89.84
DAQ					
Data Acquisition Board	Ridgeline Ins.	$23,450.00	Adlink	$2,417	$21,063.00
GPS Reference	Ridgeline Ins.	$2947.50	Quartzlock	$938.61	$2,008.89
Computer					
motherboard	ECS	$129.99	ASRock	$109.99	$20.00
Hard drive	Kingston	$499.99	Seagate	$149.99	$350.00
CPU	Intel	$118.99	Intel	$119.99	-$1.00
RAM Chipset	G.Skill	$99.99	G.Skill	$46.99	$53.00
Power Supply	FSP	$69.99	ATX miniITX	$19.99	$50.00

Solar Equipment					
Solar panels	N/A		Solartech	$156.00	-$156.00
Batteries	N/A		Local	$60.29	-$60.29
Framing Assembly					
Tubes,screws, bolts, Wachers…	McMaster	$303.94	In Home	$50	$253.94
Weatherproof Box	Hoffman	$875.00	L-Com	$335.99	$539.01
Total		$41,400.18		$8,126.79	$33,273.39

Table 8 Components price and comparison

Rogers Corporation have an university program that gives free sampler of the materials but in the table above commercial price was taken into consideration, even though there was no cost involved.

4.2 RF Characterization

To place the RF components a thick metal plate is desired in order to dissipate heat and provide physical stability to the circuit. Aluminum was the selected choice due to its properties against corrosion, low cost compared to stainless steel and the ease to drill and thread on it. That last property was very important in the decision since instead of use a commercial machine shop and ask for pre-drilled and pre-threaded aluminum plates, specifically design for the receiver circuitry, all the drilling and threading has been done at the university labs. *L-com®*, the company selected to provide the weatherproof box, allows adding to the order a pre-drilled aluminum plate. The threaded holes in the plate are placed randomly around the plate. The plate from L-Com® was selected due to price convenience. The plate with the RF Components is presented in Figure 19.

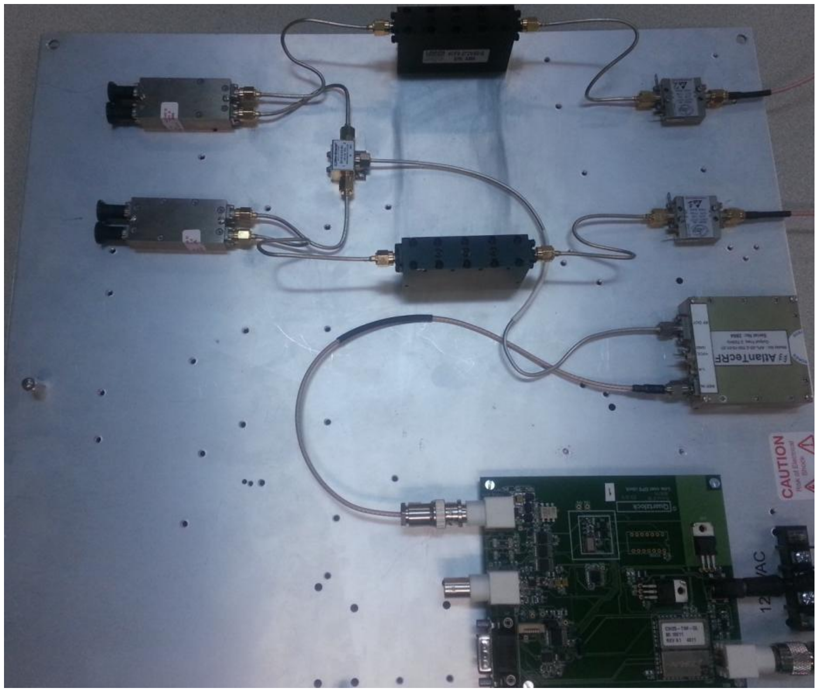

Figure 19 RF Components at the aluminum plate

The RF components where carefully selected to operate at the same DC voltage in order to feed them from only one power supply. In this case all components operate with 12V DC. This voltage will be provided by a solar power system explained later.

A characterization of the RF components was performed in order to know the exact received power the DAQ is reading. Figure 20 presents the setup where the characterization was performed.

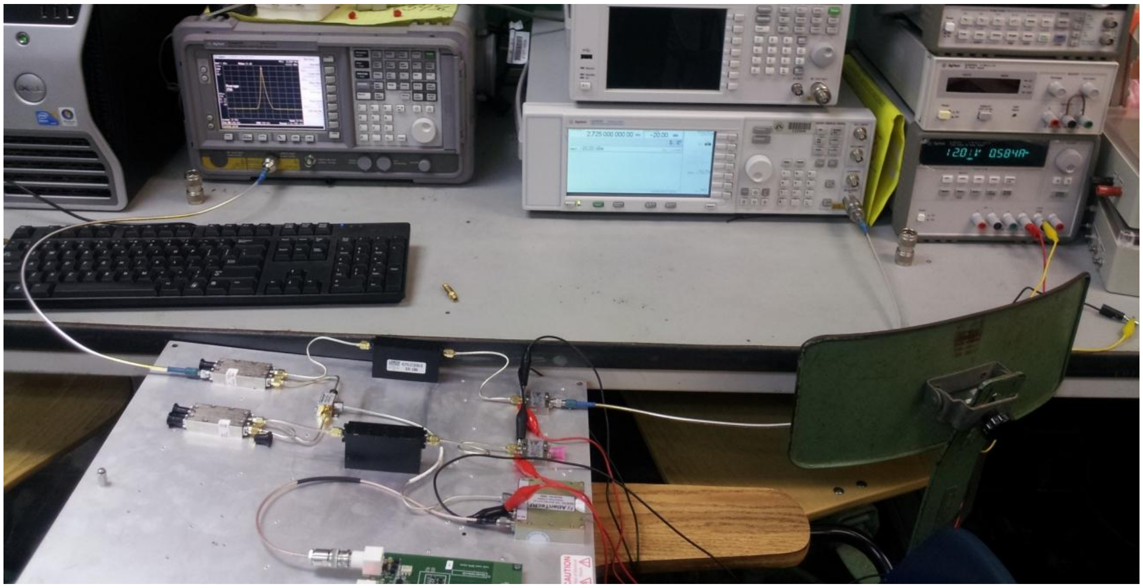

Figure 20 Receiver Characterization Setup

The 12 DC voltages was provided to the system by an Agilent Power Supply E3631A, the input power, simulating the received antenna power, is provided by a signal generator Agilent E4428C, and was measured in a spectrum analyzer Agilent E4402B. Data from the characterization is very important in order to the operator to program the DAQ system. In Table 9 is presented all detail from the characterization test. As seen in the table each channel has a different path loss that needs to be added to the card programming for the proper operation. Since it is not known the exact purpose of the receiver, due to non-disclosure policy, only a display and storage of the received signal is demonstrated in this project.

RF Testing									
Frequency	2725MHz		**Losses in testing cables**		1.28dBm				
Input Power	-20dBm								
Cables from Antenna to LNA	Cable 1	2.73dB							
	Cable 2	2.56 dB							
Component	**Channel 1**			**Channel 2**			**Nominal Values**	**Difference**	**Diff**
	Power Out (dBm)	**Losses (dB)**	**Gain(dBm)**	**Power Out (dBm)**	**Losses(dB)**	**Gain(dB)**	**(dBm)**	**dB**	**%**
PLDRO	12.78						13	0.22	1.69%
PLDRO+Cable	11.38	1.4							
PLDRO+Cable+Splitter	8.7	2.68		8.78	2.6		8.38	-0.32	3.82%
PLDRO+Cable+Splitter+Ca	8.42	0.28		8.38	0.4				
LNA	1.78		23.06	1.72		23	3	-0.06	2.00%
LNA + Cable	1.5			1.58					
LNA + Cable + Filter	0.88	0.62	22.16	1	0.58	22.28			
LNA + Cable + Filter + Cab	0.86	.02		0.93	.07				
25MHz									
Mixer Output	-5.64	6.5	15.64	-6.12	7.05	15.16			
Mixer Output + Cable	-6.09	.45		-6.68	.56				
Legend									
Green					Component providing the loss in respective line				
					Components in this color are input power independent				

Table 9 RF Components characterization

4.3 Data Acquisition System

The card was installed in the computer and tested first with a pre-loaded program that allows the user to insert a continuous 100 kHz signal, and observe that the card it is working properly, see Figure 21.

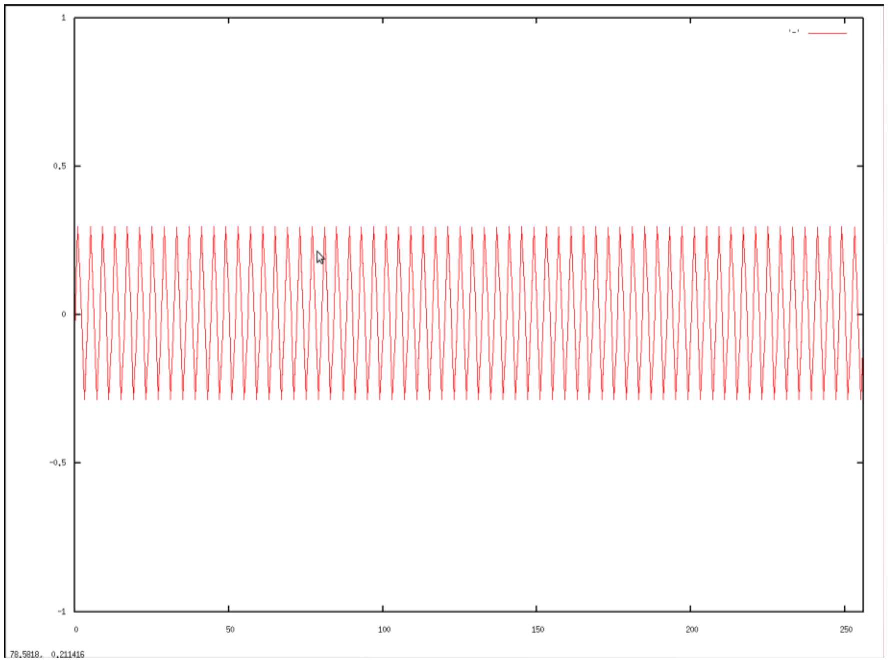

Figure 21 100KHz signal at 0dBm as plotted by PCI-9812

The pre-loaded program was then modified in order to obtain good visualization for much higher frequencies and a lower input power. At this time the signal input to the card was modulated at a frequency of 25 MHz in order to simulate the transmitter signal and to see how the visualization behaves, the results are showed in Figure 22.

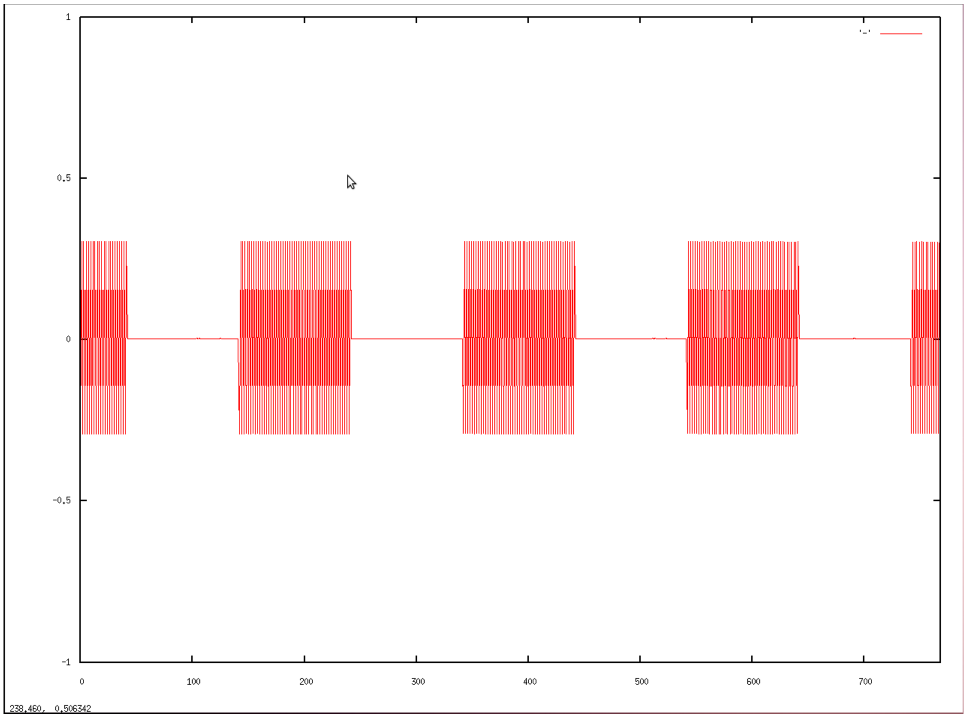

Figure 22 25MHz modulated by a 10KHz signal

4.4 Antenna

4.4.1 Antenna Construction

Satisfied with the simulations for the antenna and with the material already ordered from Rogers Corporation, the antenna construction started using the LPKF ProtoMat H100 milling machine. *CircuitCam* is the software used to import the .dxf file (CAD drawing file format) and set the machine operation. Basically this software determines how the drill will behave and which drill bit will be used in the circuit construction. Figure 23 shows the antenna drawing with all instructions already set by CircuitCam. All lines in red are where copper will stay (no rubout). All other lines are a representation of where the drill bit will be passing.

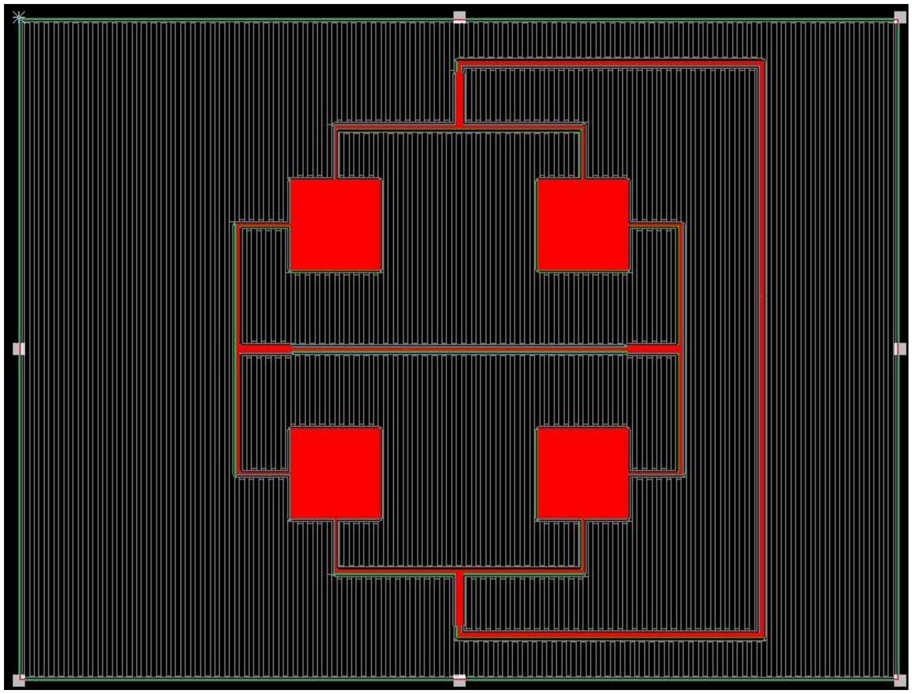

Figure 23 Antenna in CircuitCam

From CircuitCam the drawing is exported to the LPKF format and can be opened in the BoardMaster 5.1 which is the software used to control the milling machine. The screen in BoardMaster gives the area where the material is placed, have a camera that shows the fabrication process and different command buttons to manipulate the machine. Figure 24 is an image of the BoardMaster window; the selected red area is the area about to be rubout.

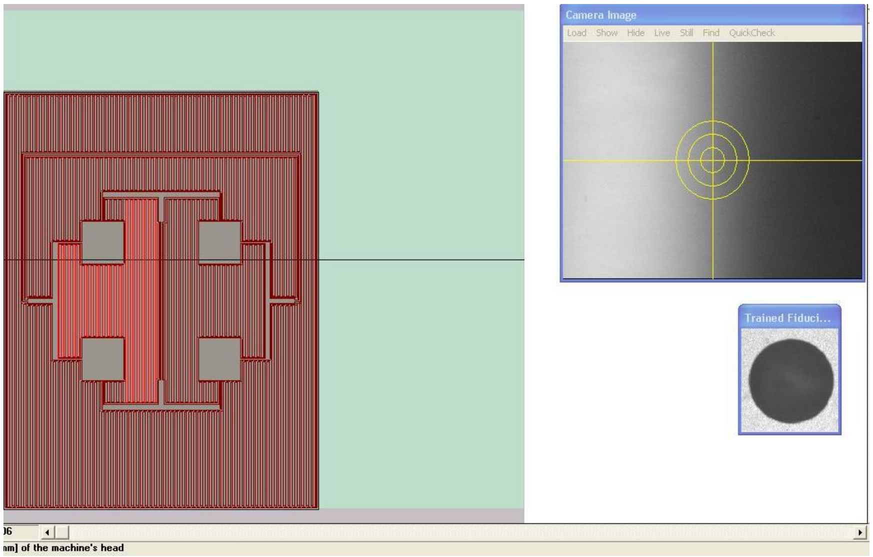

Figure 24 BoardMaster window

Figure 25 shows the antenna in progress just before the machine returns to the drill bit tray to continue with the next step. The machine was programmed to start with the smallest drill bit and finish with the largest one. In the image presented the machine has already finished with the two smallest drill bits that were used to mask the antenna and feed network. The large one was used to rubout remain copper out of the board.

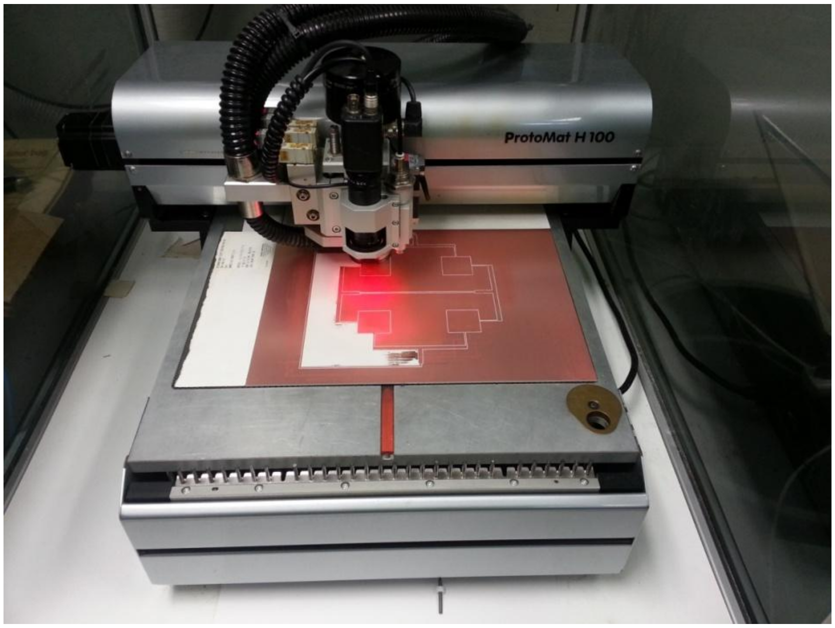

Figure 25 Antenna in progress

The LPKF milling machine completed the hardest part of the antenna which are the square patches, the lines, and the feeder holes. These are the antennas most difficult fabrication sections, because of the high precision needed. After the antenna was completed, a precision knife was then used to scrap excess copper that remained on the board. Figure 26 is the antenna completed with the extra copper at one side and the tools used to scrap it off.

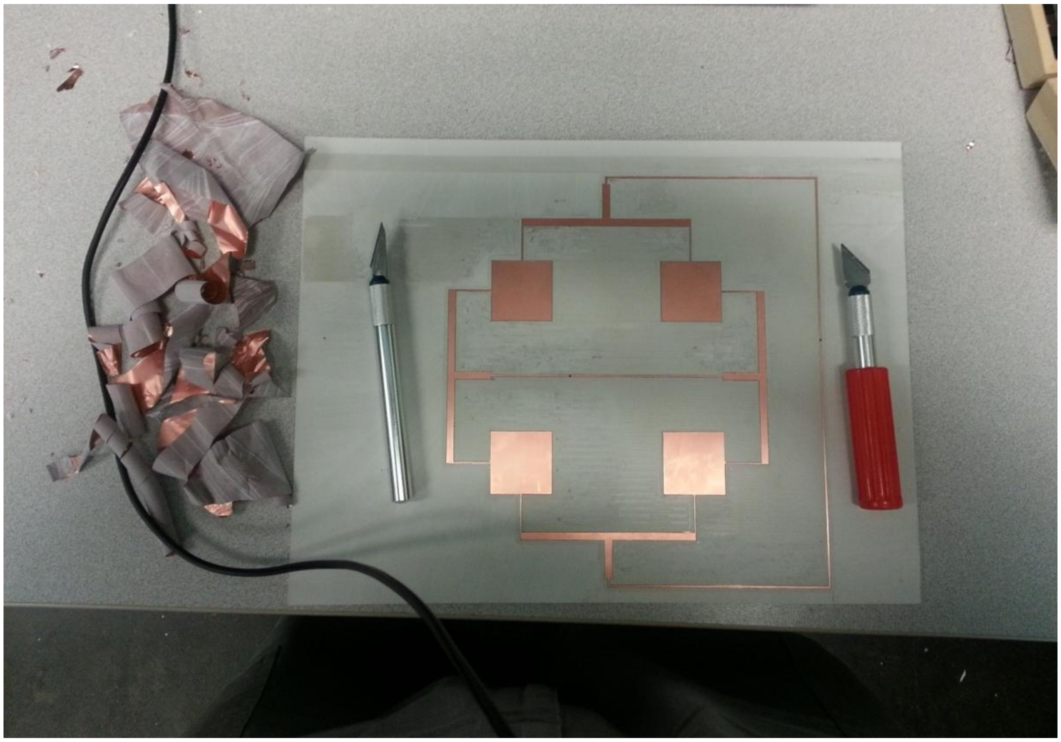

Figure 26 Antenna Completed

Operation test were performed on the constructed antenna in order to verify the operation frequency and how well the antenna was matched. Figure 27 to Figure 29 are plots from the Agilent 8719ES S-Parameter Network Analyzer. The goal for the antenna return loss was -10dB, that is the minimum required. The measured return loss for the antenna is -15dB for one channel and -17dB in the other, satisfying the expected goal. And for the port isolation measurement it exceeded the 30dB. These results are proof that the patch and matching network dimension have been constructed as simulated.

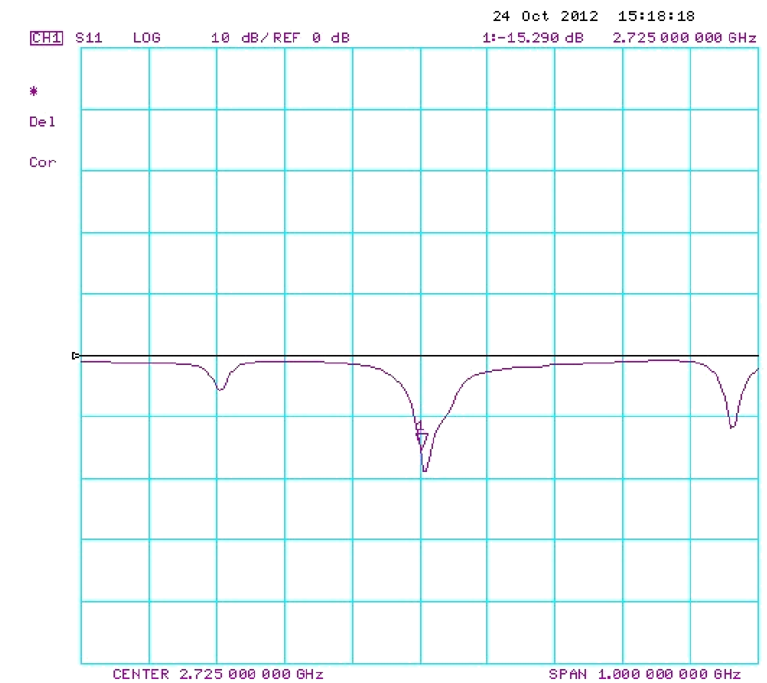

Figure 27 Horizontal polarization return loss

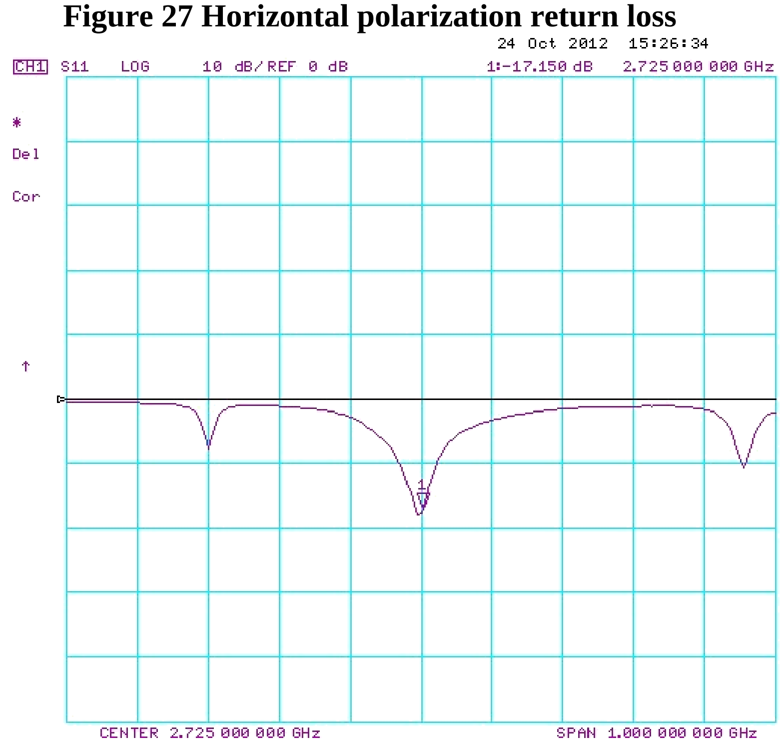

Figure 28 Vertical polarization return loss

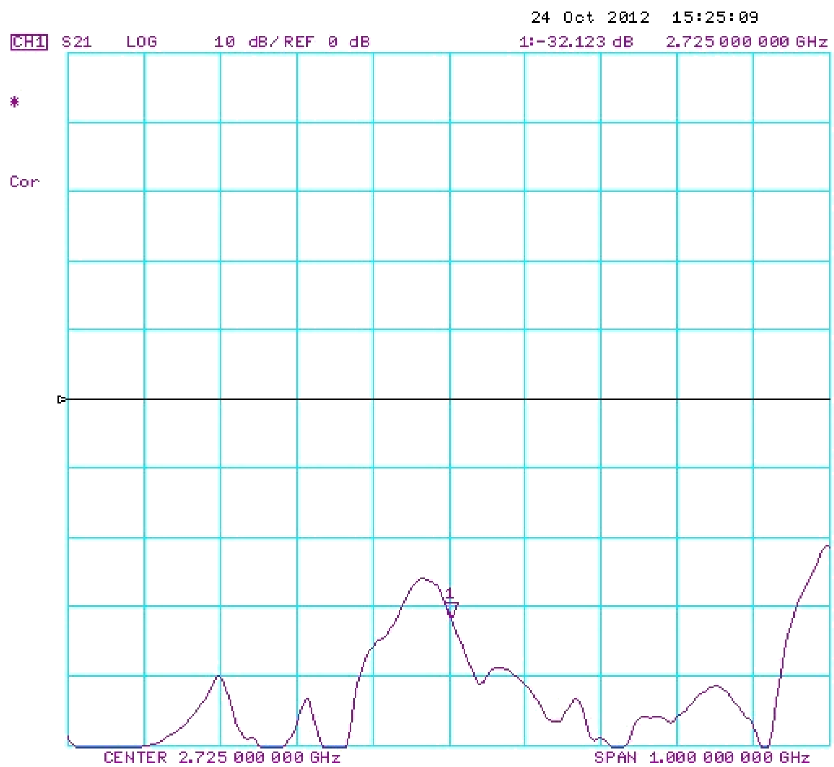

Figure 29 Antenna port isolation

Results were as expected. In simulation both return losses were close to -15dB and in measurement the result for one channel was -15dB and -17dB exceeding the simulated results.

The antenna needs to be covered from weather since this is a device intended to be outside under harsh weather conditions. For protecting the antenna, a commercially available TV antenna cover was used. The antenna was purchased and then the cover was removed to be used in the in-house antenna array.

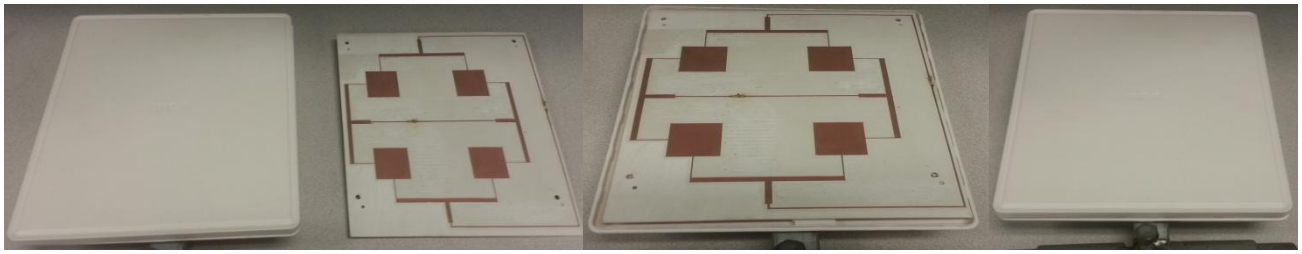

Figure 30 Antenna inside cover

After installing the antenna into the cover the test was performed again to check any variations in the performance. Results are shown in Figure 31 to 33. The return loss decreased significantly but it is still within specifications of the design. The return loss for the antenna inside the cover is around -10dB which was the original goal. The port isolation is still more than 30dB.

Figure 31 Vertical polarization return loss. (Antenna in cover)

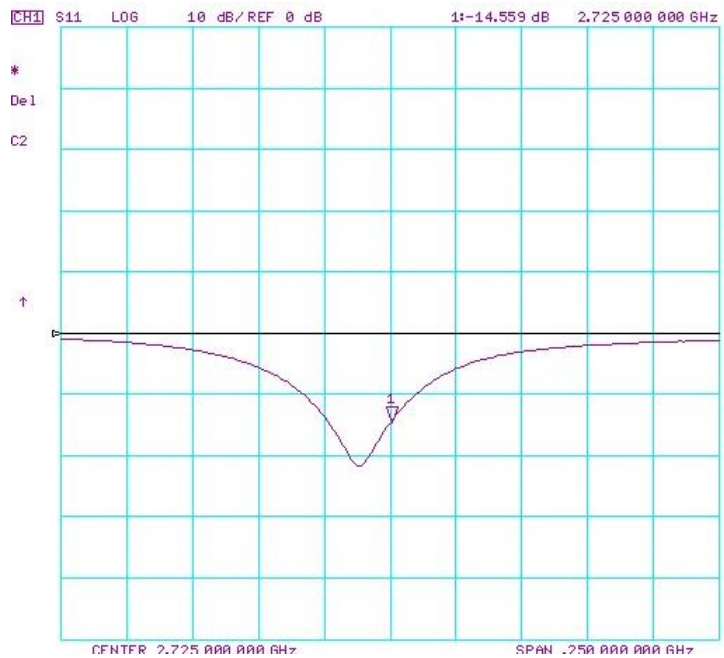

Figure 32 Horizontal polarization return loss. (Antenna in cover)

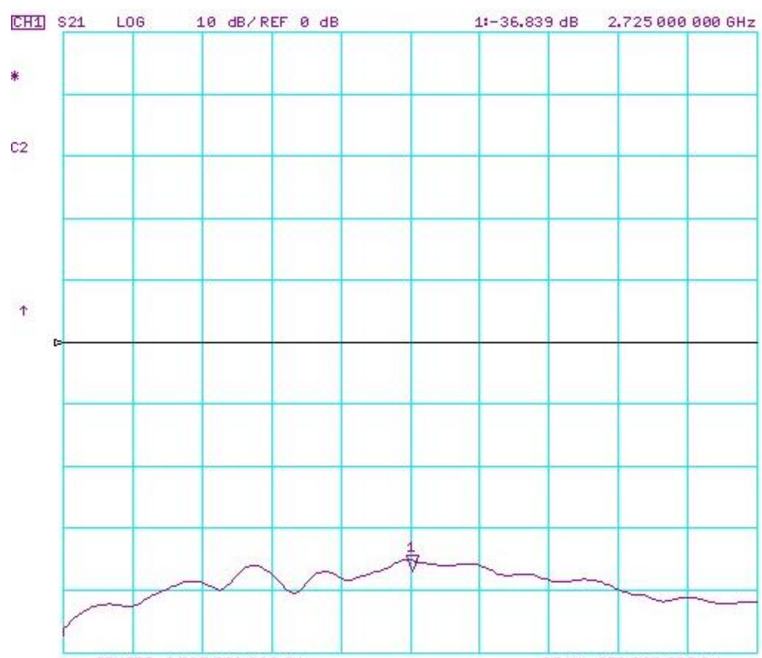

Figure 33 Antenna port isolation (Antenna in cover)

4.5 Integration and Implementation

With the RF circuit, the data acquisition system, and the stand already designed and constructed, the antenna was the last part needed for the project completion. In order to put all pieces together the weather proof box, the solar panel, and the antenna were placed in the stand.

Figure 34 Stand with antenna, weather proof box and solar panel.

The battery was placed in a Johnson box. This Johnson box is a plastic box usually used to put electrical connections in the outside, below the weather proof box. The GPS antenna was placed in a pipe and tied with presses from the box's holders. After connecting the antenna to the box through SMA cables and the solar circuit with the DC power distributor inside the box (see Figure 35) the receiver was completed and tested.

Figure 35 Receiver Completed

For the testing the receiver was placed in a parking lot near the engineering building (see Figure 37). To simulate the S-Band transmitter, a signal generator connected to an antenna was used. The antenna was available from a previous CAPSTONE project and it was slightly modified to operate at 2.725GHz (see Figure 36).

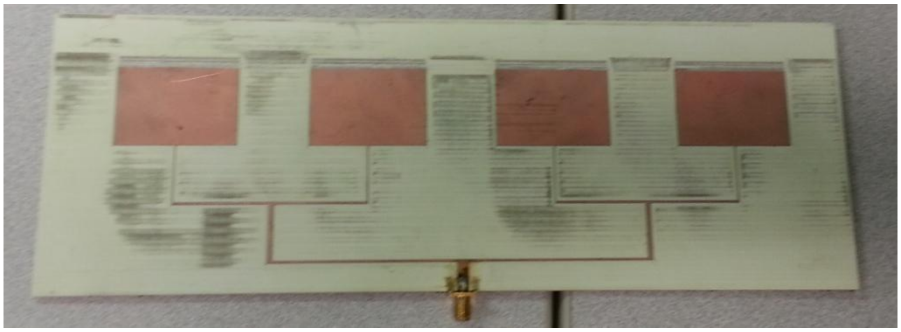

Figure 36 Transmitter antenna used for the final test

The signal generator was placed in the laboratory with the antenna pointing outside the window towards the parking lot (see Figure 38). The signal generator was set with a 2.725GHz signal modulated with a 10MHz pulse and -10dBm of output power.

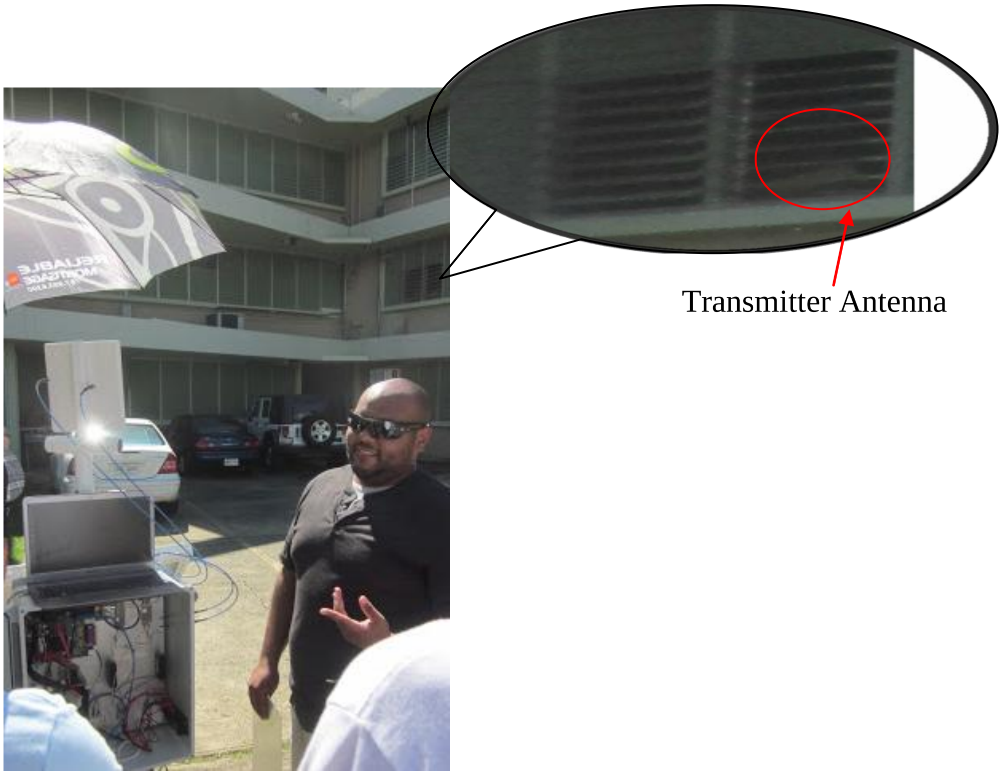

Figure 37 Transmitter's location during receiver test

In order to see the image of the data acquisition card a laptop computer was used to communicate to the receiver's computer. This images are presented in Figures 38 to 41. The images are print screens from the laptop with the real time plots generated from the receiver data acquisition system. In the figures the red line is the horizontal polarization, the green one is the vertical polarization.

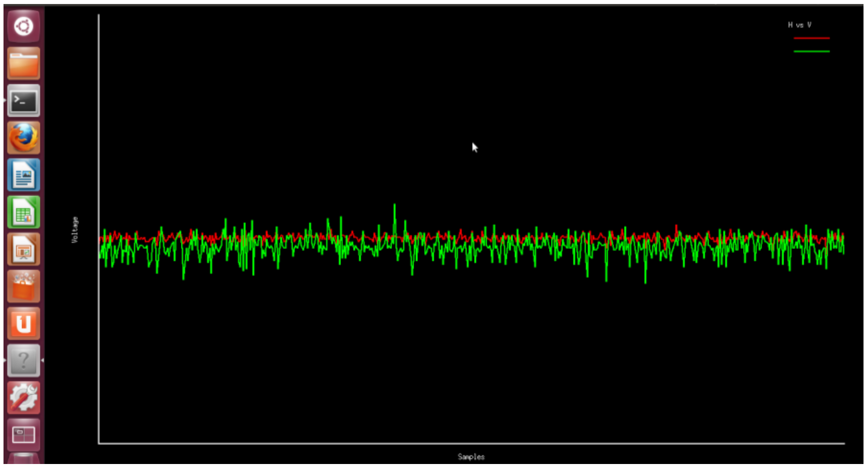

Figure 38 Receiver with the transmitter off

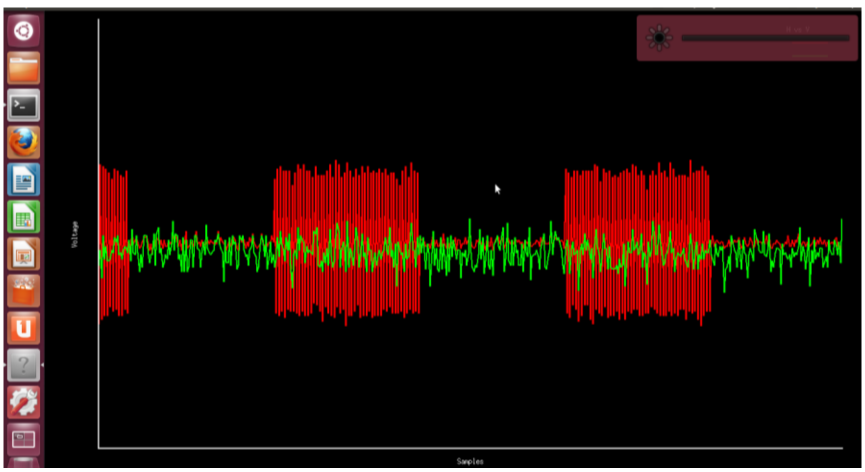

Figure 39 Transmitting horizontal polarization only

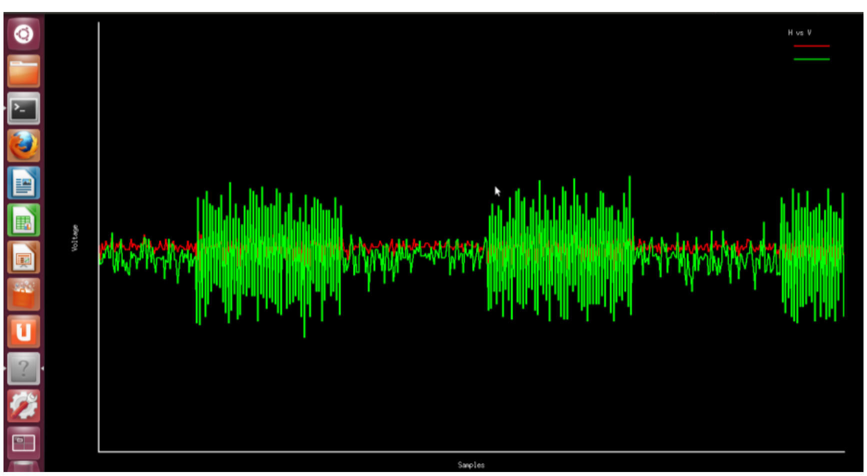

Figure 40 Transmitting Vertical polarization only

The receiver successfully detected the transmitted signal for both, horizontal and vertical channels. Since a dual polarized antenna is not available for the test, the transmitter antenna was placed in a diagonal position, that way the receiver will detect both polarizations at the same time.

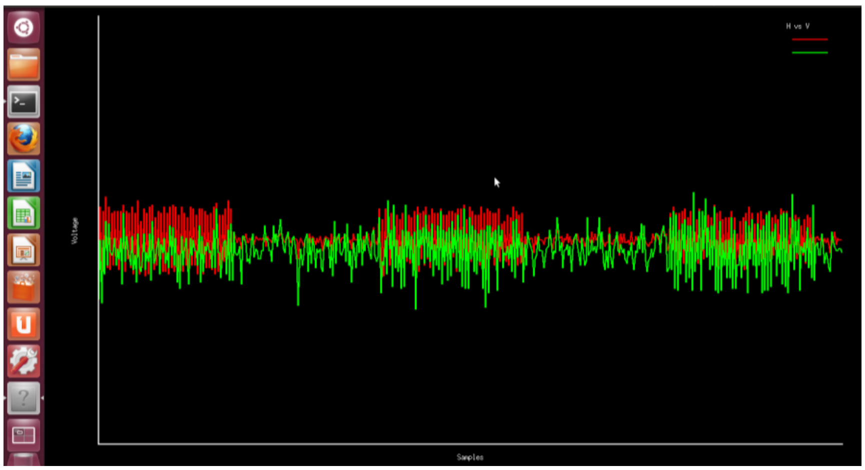

Figure 41 Transmitting horizontal and vertical at the same time

5 Conclusion and Future Work

The main objectives of this project were successfully achieved. A dual polarized, low cost, low power, easy to deploy and user friendly receiver was designed, constructed and tested.

Even when a very similar design was developed in Colorado State University (CSU) with University of Puerto Rico Mayagüez Campus (UPRM) collaboration, this design has its own features that make it unique. Some of these features are a PCI data acquisition system, low cost, and solar powered.

The components were selected carefully, and special consideration was taken to fabricate some of the parts of the receiver in Campus. These efforts allow us to construct and test the receiver under the ten thousand dollars budget. The dual polarization was achieved with a dual polarized microstrip antenna, two different channels for each polarization channel in the RF circuit, and with a dual channel data acquisition card that have the capability to manage two different signals at the same time and at the same velocity. Low power consumption computer and devices were used to control the receiver in order to use a solar system to power the device.

Each component and individual system has been tested with satisfactory results. The overall test was a success by properly showing that the receiver system is working. Although the receiver works as expected, the tests made for this project purposes just gives the end user the guarantee that the whole system is properly working.

The receiver system needs a program to be developed by the end user, to control the data acquisition card, which allows the user to exploit the system capabilities like Doppler detection, among others. The mentioned program can be done in C++, LabView or Matlab. The C++

program that is delivered with this project is just for test purposes, and it is not intended to be a program for target detection. Because of time limitation the PCI-9820, was not tested. If possible that card should be bought in order to increase resolution for target detection, upgrade to a newer operative system and make easier the programming for target detection.

If possible in order to decrease the losses, the user can make the coaxial cables that go from the antenna to the weather box shorter in order to have an optimized length, but the length the cables have at this moment allows the antenna to rotate 360 degrees.

Receiver stand is completely detachable and in the user manual that will be delivered with the receiver will be a set of instructions of how to put it together. This is why every single piece will be identified with a label that will make easy the assembly process.

REFERENCES

[1] Willis N. J. *Bistatic Radar*. Scitech, New York 2005

[2] Glaser, J.I.: ‘Fifty years of bistatic and multistatic radar’, IEE Proc. F, 1986, 133, (7), pp. 596–603

[3] Willis, N.J.; Griffiths, H.D.; , “Advances in bistatic radar (Willis, N.J. and Griffiths, H.D., Eds.; 2007) [Book Review],” *Aerospace and Electronic Systems Magazine, IEEE* , vol.23, no.7, pp.46, July 2008

[4] Griffiths, Hugh; , “New directions in bistatic radar,” *Radar Conference, 2008. RADAR’08. IEEE* , vol., no., pp.1, 26-30 May 2008

[5] Griffiths, H.; Willis, N.; , “Klein Heidelberg—The First Modern Bistatic Radar System,” *Aerospace and Electronic Systems, IEEE Transactions on* , vol.46, no.4, pp.1571-1588, Oct. 2010

[6] Griffiths, H.D.; , “From a different perspective: principles, practice and potential of bistatic radar,” *Radar Conference, 2003. Proceedings of the International* , vol., no., pp. 1-7, 3-5 Sept. 2003

[7] Cherniakov M. *Bistatic Radar Principles and Practice* , Wiley, John and Sons Inc., 2007

[8] Zahn, D.; Sarabandi, K.; , “Simulation of bistatic scattering for assessing the application of existing communication satellites to remote sensing of rough surfaces ,” *Geoscience and Remote Sensing Symposium, 2000. Proceedings. IGARSS 2000. IEEE 2000 International* , vol.4, no., pp.1528-1530 vol.4, 2000

[9] Skolnik, M.I.: ‘Introduction to radar systems’ (McGraw-Hill, New York, 1980)

[10] Pozar, D.M., Microwave Engineering, 2nd ed., Wiley: New York, 1998.

[11] Vega M., Student Developed Meteorological Radar Network for the Western Part of

Puerto Rico: First Node., M.S. Thesis, University of Puerto Rico at Mayaguez, 2007

[12] Weib, M.; , “Synchronisation of bistatic radar systems,” *Geoscience and Remote Sensing Symposium, 2004. IGARSS ‘04. Proceedings. 2004 IEEE International* , vol.3, no., pp. 1750- 1753 vol.3, 20-24 Sept. 2004

[13] Huang Yulin; Yang Jianyu; Xiong Jintao; , “Synchronization Technology of Bistatic Radar System,” *Communications, Circuits and Systems Proceedings, 2006 International Conference on* , vol.4, no., pp.2219-2221, 25-28 June 2006

[14] Johnsen T. Erik Olsen K., Bi-and Multistatic Radar, Norwegian Defense Research Establishment

[15] K. E. Olsen, S. Johnsrud, T. Johnsen, P. Sørnes, I. Tansem, H. Bjordal, L. W. Westad, “Results from an experimental Continuous Wave Low Probability of Intercept Bistatic Radar – The first experiments”, Proc. IEE Int. Radar Conf., Toulouse, France, 2004.

[16] E.W. Weisstein, Cassini Ovals, MathWorld—A Wolfram Web Resource, http://mathworld.wolfram.com/CassiniOvals.html.

[17] Thabet, A.; El Dein, A.Z.; Hassan, A.; , “Design of compact microstrip antenna by using new nano-composite materials,” *Nanoelectronics Conference (INEC), 2011 IEEE 4th International* , vol., no., pp.1-2, 21-24 June 2011

[18] Sabban, A.;”Applications of MM Wave Microstrip Antenna Arrays,” *Signals, Systems and Electronics, 2007. ISSSE ‘07. International Symposium on* , vol., no., pp.119-122, July 30 2007-Aug. 2 2007

[19] David M. Pozar, “Microstrip Antennas”, IEEE Proceeding, Vol. 80, No. 1, Jan 1992

[20] Marrero V., Dual Polarized Microstrip Antenna Array For the Off-The_Grid Radar., M.S. Thesis, University of Puerto Rico at Mayaguez, 2007.

[21] ANSI/IEEE Standard Test Procedures for Antennas, ANSI/IEEE Std. 149-1979, IEEE, New York; John Wiley Distributors.

[22] “Lecture 15: Linear Array Theory – Part 1”, Universidad Técnica Federico Santa Maria, Chile.

[23] Rauch T. Stacking_Broadside_Collinear.w8ji.com. [retrieved] October 28, 2012, from http://www.w8ji.com/stacking_broadside_collinear.htm

[24] Radiation Characteristics, Prediction Pattern for HF Horizontal,

http://www.moonraker.com.au/techni/patterns2.htm

[25] C. Balanis, *Antenna Theory: Analysis and Design*, 2nd Ed, Wiley, 1997.

[26] Junyent Francesc, “eDaq1b Radar Data Acquisition System”, http://www.rli-radar.com/rli/hardware/edaq1b/index.html

[27] Jim Dunlop, Photovoltaic Systems, second edition, American Technical Publishers, INC., Illinois, 2010

[28] Saarijarvi Mirva, “Art of comparing RFID reader power outputs”, http://rfidarena.com/2011/9/19/art-of-comparing-rfid-reader-power-outputs.aspx, September 2012

[29] Bringi, V.N., and V. Chandrasekar, Polarimetric Doppler Radar, 1st ed., Cambridge University Press: Cambridge, UK, 2001.

APPENDIX A. SOLAR CALCULATION TABLES

The student Jose D. Diaz did this Excel program that gives the necessary equipment for the solar circuit. In the following tables are presented the power consumption of the receiver and the total of batteries and solar panels needed to satisfy the consumption.

Input Data				
Electric Load Estimation Watt-hrs/day				
AC Average Daily Load	**DC Average Daily Load**	**DC Total Connected Watts**	**AC Total Connected Watts**	
0	60	60	0	
Solar Panels Specifications				
Vmp	**Imp**	**Voc**	**Isc**	**Nominal Voltage**
18.18	3.1	22.1	3.31	12
Inverter		***Charge Controller Specifications***		
Efficiency		**CC Watt Rating**	**Max PV Array Open Circuit Voltage Allowed**	
0.85		2500	150	

Battery Sizing Worksheet

AC Average Daily Load (W-hr/day)	Inverter Efficiency	DC Average Daily Load (W-hr/day)	DC System Voltage	Average Amp-hours/day
0	0.85	60	12	5.00
Average Amp-hours/day	**Days of Autonomy**	**Discharge Limit**	**Battery AH Capacity**	**Batteries in parallel**
5.00	2	0.5	20	1.00
DC System Voltage	**Battery Voltage**	**Batteries In Series**	**Batteries In Parallel**	**Total Batteries**
12	12	1	1.00	1.00

Array Sizing Worksheet

Average Amp-hrs/day	Battery Efficiency	Peak Sun Hrs/day (PR)	Array Peak Amps
5.00	0.8	4	1.56
Array Peak Amps	**Peak Amps/module**	**Modules In Parallel**	**Module Short Circuit Corrent**
1.56	3.1	0.50	3.31

DC System Voltage	Nominal Module Voltage	Modules In Series	Modules In Parallel	Modules Total:
12	12	***1***	***0.50***	***0.50***

Controller Sizing Worksheet

Module Short Circuit Current	Modules In Parallel	Safety Factor	Array Short Circuit Amps	Controller Array Amps
3.31	0.50	1.25	2.09	2
DC Total Connected Watts	**DC System Voltage**	**Maximum DC Load Amps**	**Controller Load Amps**	
60	12	5	5	

Stand Alone Array & Controller With MPPT Sizing Worksheet

Total Daily Load	Peak Sun Hours Per Day	Battery Efficiency	PV Temp Loss	Derate Factor
60	4	0.8	0.88	0.85
PV Array Watts	**STC Watt Rating**	**Number of Modules Needed**	**Max Watss Charge Controller Must Pass**	

25.06684492	56.358	0.444778823	25.06684492
Array Nominal Voltage	**PV Module Nominal Voltage**	**#of Modules Required in Series**	**Charge Controllers Needed**
12	12	1	0.010026738
Maximum PV Voltage			
26.52			

APPENDIX B C++ PROGRAM FOR ADLINK PCI-9812

```
/*
 *  RealtimePlot - get data from the acquisition card and plot it
 *                 realtime with gnuplot
 *
 *
 */




#include <stdio.h>
#include <stdlib.h>
#include <unistd.h>
#include "dask.h"
#include "conio.h"





U16 channel=1;  //4 channels
U16 range=AD_B_1_V;
char *file_name="9812dat.txt";
U32 read_count=1024, mem_size = 0;
F64 sample_rate=2000000;
I16 * ai_buf;
double* ai_buf2;

FILE *gp_o;


BOOLEAN write_to_file( U16 *buf, int num_chan );
void show_channel_data( double *buf, int num_chan );
void writeForGnuplot(double *buf,int channel);

int main(void)
{
    I16 card, err;

    setbuf( stdout, NULL );
    printf("This program inputs %ld data from CH-0 to CH-%d of PCI-
9812 in %d Hz, and\nstore data to file '%s'.\nPlease press any key to
start the operation.\n", read_count, channel, (int)sample_rate,
file_name);

    getch();
```

```
    if ((card=Register_Card (PCI_9812, 0)) <0 ) {
        printf("Register_Card error=%d\n", card);
        exit(1);
    }
    err = AI_9812_Config(card, P9812_TRGMOD_SOFT, P9812_TRGSRC_CH0,
P9812_TRGSLP_POS, P9812_AD2_GT_PCI|P9812_CLKSRC_INT, 0x80, 0);
    if (err!=0) {
        printf("AI_9812_Config error=%d", err);
        exit(1);
    }
    err = AI_AsyncDblBufferMode(card, 0);
    if (err!=0) {
        printf("AI_DblBufferMode error=%d", err);
        exit(1);
    }

    mem_size=read_count * 2;
    ai_buf = (I16*)malloc(mem_size);
    ai_buf2 = (double*)malloc(read_count*sizeof(double));

    gp_o = popen("gnuplot","w");
    fprintf(gp_o,"set terminal x11 0\n");
    fprintf(gp_o,"set yr [-0.05:0.05]\n");
    fprintf(gp_o,"set xr [0:512]\n");
    fprintf(gp_o,"set object 1 rectangle from screen 0,0 to screen 1,1
fillcolor rgb \"black\"  behind\n");
    fprintf(gp_o,"set xlabel 'Samples' textcolor rgb 'white' font
\"Vera,16\"\n");
    fprintf(gp_o,"set ylabel 'Voltage' textcolor rgb 'white'font
\"Vera,16\"\n");
    fprintf(gp_o,"set key  title 'H vs V' textcolor rgb 'white'\n");
    fprintf(gp_o,"set border 3 ls 2 lw 2 lc rgb 'white'\n unset ytics
\n unset xtics \n");


    while(1)
      {
    err = AI_ContScanChannels(card, channel, range, ai_buf,
read_count, sample_rate, SYNCH_OP);
    if (err!=0) {
        printf("AI_ContReadChannel error=%d", err);
        free( ai_buf );
        Release_Card(card);
        exit(1);
    }
    int count1;
    AI_ContVScale(card,range,ai_buf,ai_buf2,read_count);
    AI_AsyncClear(card,&count1);
```

```
    printf(" %ld data trnasfered !\n", read_count );



    //if( write_to_file( (U16*)ai_buf, channel+1 ) )
    //    printf("\n\nThe input data is already stored in file
'%s'.\n", file_name);

    //show_channel_data( (double*)ai_buf2, channel+1 );
    writeForGnuplot(ai_buf2,channel+1);
    //usleep(250000);

      }

    free( ai_buf );
    Release_Card(card);
    printf("\nPress ENTER to exit the program. "); getch();
putchar('\n');
    return 0;
}


BOOLEAN write_to_file( U16 *buf, int num_chan )
{
    // int chan_no;
    U8 temp_s[100];
    FILE *fp;
    U32 i;

    if (( fp = fopen( file_name , "w+b")) == NULL)
        return FALSE;


    for(i=0; i<read_count; i+=num_chan){
        sprintf( temp_s, "%04x   %04x   %04x   %04x\n", buf[i],
buf[i+1], buf[i+2], buf[i+3] );
        fwrite(temp_s, sizeof(U8), strlen(temp_s), fp);
    }

    fclose( fp );
    return TRUE;
}

void writeForGnuplot(double *buf,int channel)
{
  int i =0;
```

```
  /*  FILE *fp;

  if((fp = fopen("gplot.txt","w+b")) == NULL)
    return FALSE;

  for (i=0;i<read_count;i++)
    {
      fprintf(fp,"%d\t%f\n",i,buf[i]);
    }

    fclose(fp);*/

  int index=0;
  int value =0;
  fprintf(gp_o,"plot '-' with lines lw 2 , '-' with lines lw 2\n");
  //realtime

  for (i=0;i<read_count;i++)
    {
      if( i % 2 == 0)
     {
       fprintf(gp_o,"%d\t%f\n",value,buf[i]);
       value++;
     }

      index++;
    }

  fprintf(gp_o,"e\n");
  value = 0;
  for(i=0;i<read_count;i++)
    {
      if(i % 2 == 1)
     {
       fprintf(gp_o,"%d\t%f\n",value,buf[i]);
       value++;
     }
      index++;
    }

  fprintf(gp_o,"e\n");
  usleep(10000);
  return TRUE;

}

void show_channel_data( double *buf, int num_chan )
{
```

```
    double adinput;
    int channel_no, chan_idx;
    U32 i, k;

    for( chan_idx = 0; chan_idx< num_chan; chan_idx++ ){
        printf(" >>>>>>>>>>>>>>> the first 240 data from Channel#%d
<<<<<<<<<<<<<<< \n", chan_idx+1 );
        for( i = 0, k=0; i< read_count && k< 240 ; i++ ){
            adinput = buf[i];
            channel_no = i% num_chan;
            //adinput = adinput >>4;

            if( channel_no == chan_idx ){
                printf("%f  ", adinput );
                if( (k+1)%12 == 0 )
                 putchar('\n');
                k++;
            }
        }

        if( chan_idx < num_chan -1 ){
            printf("press any key for next channel:\n");getch();
        }
    }
}
```

APPENDIX C GPS REFERENCE SPECIFICATIONS

1. Quartzlock Products

   a. **E8-X**

      i. The Quartzlock E8-X is a breakthrough in exceptionally low cost, miniature, traceable, calibration-free, off-air frequency & time standards. These references maintain the high frequency & time accuracy required for demanding applications.

   b. **Features**

      i. Low distortion 10MHz Sine & 1PPS outputs

      ii. <8x10-13…..5x10-14 accuracy

      iii. No drift

      iv. High stability nationally & internationally

      v. 1 year warranty

      vi. Lowest cost available

      vii. Very long production life & support. Quartzlock's 2A LF tracking RX (E8-X GPS predecessor) series has been in production for >30 years

      viii. Many versions of the E8-X GPS DO are available. PCB, mil, low and ultra low noise E8-Y.

   c. **Benefits**

      i. No calibration required

ii. Traceable reference

d. **Applications**

i. Calibration of counters, frequency meters, spectrum & network analysers

ii. Synthesizers, & communication analysers

iii. Reference for: VHF, UHF & PMR TX, CDMA, Tetra, DTV & DAB

iv. Production test frequency standard

v. Network time protocol use in financial, utilities, security & communications timing

vi. OEM

vii. Standard for calibration labs, radio workshops, labs and stations

e. **Quality**

i. Quartzlock's hydrogen maser based laboratory is used in production test & quality assurance to ensure compliance with offset and stability specifications.

ii. Standard Specification:

Output Frequency	10MHz
Output Level	12dBm
1PPS Output	1
Number of Outputs	1
STS1s	2x10-10
STS10s	4x10-10
STS100s	5x10-11
STS1000s	2x10-11
Phase Noise 1Hz	60dBC
Phase Noise 10Hz	90dBC
Phase Noise 100Hz	115dBC
Phase Noise 1kHz	130dBC
Phase Noise 10kHz	140dBc
Warm Time	15min

PSU Nominal	12V
PSU Min	6V
PSU Max	14V
Current	250mA
Supply	DC